



Trongino

LIBRARY Michigan State University

This is to certify that the

thesis entitled
TEMPERATURE STUDIES OF WATER VAPOR
ADSORPTION ON SILICA GEL IN
EXTERNALLY APPLIED DC ELECTRIC FIELDS

presented by

MARK WILLIAM GRENFELL

has been accepted towards fulfillment of the requirements for

Master of Science degree in Chemical Engineering

Major professo

Dr. Bruce W. Wilkinson

Date _11/10/88

MSU is an Affirmative Action/Equal Opportunity Institution

O-7639



RETURNING MATERIALS:
Place in book drop to remove this checkout from your record. FINES will be charged if book is returned after the date stamped below.

TEMPERATURE STUDIES OF WATER VAPOR ADSORPTION ON SILICA GEL IN EXTERNALLY APPLIED DC ELECTRIC FIELDS

By

Mark William Grenfell

A THESIS

Submitted to
Michigan State University
in partial fulfillment of the requirements
for the degree of

MASTER OF SCIENCE

Department of Chemical Engineering

1988

ABSTRACT

TEMPERATURE STUDIES OF WATER VAPOR ADSORPTION ON SILICA GEL IN EXTERNALLY APPLIED DC ELECTRIC FIELDS

By

Mark William Grenfell

This thesis investigated the temperature change of silica gel during water vapor adsorption in the presence of a DC electric field. Someshwar and Wilkinson (21) found that the adsorption rate of water vapor on Chromatographic Grade Silica Gel could be enhanced in the presence of non-uniform DC electric fields, while the total amount adsorbed remained constant. Isothermal conditions were assumed in the silica gel and the rate enhancement was concluded to be totally the result of the effects of the electric field. The purpose of this thesis was to investigate the isothermal assumption and to separate the electrical and the adsorption heat effects to determine if increased diffusion rates, due to electrical heating, appeared as enhanced adsorption rates. The rate of water vapor adsorption was confirmed to increase in the presence of an electric field for high gas saturation levels. measured silica gel temperature rises of three to four degrees Celcius were shown to be due primarily to the heat of adsorption, rather than electrical heating.

ACKNOWLEDGMENTS

I would like to thank Dr. Bruce W. Wilkinson for his technical and creative assistance, and especially for his patience, during the completion of this thesis.

TABLE OF CONTENTS

LIST OF	TABLES	vi
LIST OF	FIGURES	/ii
NOTATIO	vi	iii
Chapter		
I	Introduction	1
	A. Motivation for This Research B. Research Objective and Outline	1 3
II	Background and Theory	4
	 A. Heat of Adsorption B. Basis for this Work C. Current Research Thermal Effects Adsorption Rate Enhancement Using Electric Fields 	4 9 13 13
	D. Energy Balance E. Relaxation Field Discussion	20 22
III	Experimental Equipment and Experimental Procedure	24
	A. Description of the Flow Scheme B. Detailed Equipment Descriptions 1. Evaporative Water Loss Unit	25 29
	(Demco Model Z-1334) 2. The Adsorption Chamber C. Data Acquisition	29 33 34
	 Adsorption Data Temperature Data Use of Data 	34 35 36
	D. Experimental Procedure 1. General Procedure Prior to the Start of All Experiments	37 37
	 Procedure Number One Temperature Experiments Procedure Number Two 	37
	3. Procedure Number Two	30

Chapter

IV	Experimental Results	40
	A. Experiments in the Absence of an Electric Field on S-2509 Silica Gel	41
	B. Experiments in the Presence of an	
	Electric Field on S-2509 Silica Gel	4 5
	C. Comparison of the Field and Non-field Experimental Results	4.8
	D. Experiments on S-4133 Silica Gel	55
v	Discussion of Experimental Results	59
	A. Discussion of Results for S-2509	5 0
	Silica Gel B. Discussion of Results for S-4133	59
	Silica Gel	66
VI	Conclusions	68
VII	Recommendations	73
APPENDI	CES	
Append	lix	
A	Silica Gel Energy Balance	79
В	Determination of UA from Experimental Data	81
С	Prediction of the Temperature Rise for the Moist Gas Stream	83
	NOISC Gas beleam	03
D	Calculation Showing How the Pressure Drop Across the EWLU Reduced p/p _o	84
E	Calculation Showing the Silica Gel Temperature	
	Rise Due to the Electric Field in the Absence of Adsorption	85
F	Raw Data	86
BIBLIOG	RAPHY	92

LIST OF TABLES

4.1	Properties of S-2509 Silica Gel	41
4.2	Maximum Silica Gel Temperature Increase $(V = 0 \text{ kV})$	42
4.3	Maximum Silica Gel Temperature Increase $(V = 6 \text{ kV})$	46
4.4	Maximum Silica Gel Temperature Increase	49

LIST OF FIGURES

2.1	Adsorption Isotherm for Silica Gel S-2509; Amount Adsorbed (W) vs. Fraction of Total Saturation (p/p_0) ; $T = 25$ °C.	11
2.2	Adsorption of Water Vapor on Silica Gel S-2509 for $V = 0$ kV and $V = 6$ kV; $p/p_0 = 0.9$, $T = 25$ C.	12
3.1	Schematic Diagram of Experimental Flow Arrangement.	26
3.2	The Adsorption Chamber.	28
3.3	Function of the Evaporative Water Loss Unit.	30
3.4	Evaporative Water Loss Unit Calibration Curve.	32
4.1	S-2509 Silica Gel Temperature Change with $V = 0 \text{ kV}$.	44
4.2	S-2509 Silica Gel Temperature Change with $V = 6 \text{ kV}$.	47
4.3	S-2509 Silica Gel Temperature Change with $p/p_0 = 0.9$.	50
4.4	S-2509 Silica Gel Temperature Change with $p/p_0 = 0.8$.	51
4.5	S-2509 Silica Gel Temperature Change with $p/p_0 = 0.7$.	52
4.6	S-4133 Silica Gel Temperature Change with $p/p_0 = 0.9$; $V = 0$ and 3.5 kV.	56
7.1	Loss Tangent vs. Frequency for Liquid Water at 25 OC.	76

NOTATION

Area for heat transfer.

Α

 M_{o}

 M_r

M_

V=0.

O

b Function of the sample size. Charged layer superscript. С Concentration of the diffusing species. $C_{\mathbf{d}}$ Heat capacity of the solid. $C_{\mathbf{p}}$ Specific heat of the moist air. Cpair Specific heat of the silica gel. Cpsq Н Heat of adsorption. Heat of adsorption. Hads Isosteric heat of adsorption. Hst H, Integral heat of adsorption. H Differential heat of adsorption. Ι Electric field current. J Mass flux. Mass of silica gel sample. MSG m ads Adsorption rate of water onto silica gel. \dot{m}_{air} Mass flow rate of moist air. M Molecular weight of vapor being adsorbed.

Molecular weight of reference substance.

Superscript indicating local electric field is zero,

Initial solute in the solid.

Final solute in the solid.

p Polarized layer superscript.

p_v Vapor pressure of adsorbate.

p Equilibrium partial pressure of adsorbate.

 p/p_0 Fraction of total saturation in the moist air

stream.

P System pressure.

R Gas constant.

t Time.

T Temperature.

Tair Temperature of moist air.

To Initial temperature.

 T_{sq} Temperature of the silica gel.

 T_{sga} Temperature difference between the silica gel and the moist air.

U Overall heat transfer coefficient.

V Electric field potential.

x Adsorbate concentration.

z Direction of gradient subscript.

W Mass of adsorbate per mass of adsorbent.

Greek Letters

Y Diffusing species subscript.

Fraction of surface covered by adsorbed molecules.

 λ A phenomenological coefficient.

 $\lambda_{\scriptscriptstyle T}$ Latent heat of vaporization of the reference substance at the same temperature.

 μ_{γ} Chemical potential of the diffusing species.

Introduction

A. Motivation for This Research

In the technology of electrostatic precipitation, high particulate electrical resistivities reduce collection efficiencies. The resisitivity of effluent gas ash is not only a function of the chemical composition of the combustion fuel burned, but also a function of the flue-gas composition. Ash resistivity is capable of being significantly lowered through increased water vapor concentrations in the flue-gas and through the use of conditioning agents such as sulphur trioxide and some sodium compounds which bind the water more strongly on the particulate surface. (20)

The basis for this research is the continued study of the electrical effects of water vapor adsorption onto silica gel. Someshwar and Wilkinson (21) found that the adsorption rate of water vapor onto Chromatographic Grade Silica Gel could be enhanced in the presence of non-uniform DC electric fields, while the total amount of adsorbed material remained constant. Isothermal conditions were assumed in the silica gel and the rate enhancement was concluded to be totally the result of the electric field. It is not altogether clear why electric fields enhance

adsorption processes, but Someshwar (20) found adsorption rate enhancement for water adsorbate, a polar molecule, and did not see enhancement for non-polar CCl₄. In addition, Lincoln and Olinger (16) did not see adsorption rate enhancement for non-polar H₂, but did realize electric field enhancement for ethylene adsorbate. Therefore, it is possible that the adsorbate polarity may affect its activity in an electric field.

The electric field gradients in the silica gel pores, resulting from the externally applied electric field, are very large and therefore able to act on dipolar molecules. It is postulated that the force introduced on the dipolar molecules will act to enhance the rate of adsorbate flux through the adsorbent pores, thus increasing adsorption rates. (21)

when viewed in the light of the isothermal assumption, one very important consideration arises regarding the adsorption rate enhancement in the presence of the electric field. If the isothermal assumption is invalid and the silica gel temperature increases due to current flow or electrical conduction, this may enhance the diffusion process and be responsible for the adsorption rate increases rather than the applied electrical potential. On the other hand, increased temperatures should increase the partial pressure of the water above the silica gel surface and reduce the adsorption rate. Most diffusion and adsorption studies assume isothermal

conditions within the adsorbent sample. However, if heats of adsorption are high, or if electric currents are substantial in the presence of an electric field, large temperature rises may occur. Kmiotek, Wu and Ma (12) observed up to 84.7 °C temperature rises during the sorption of methanol in ZSM-5 Zeolite. If temperature rises are substantial, the initial rate period will be unaffected, until the change from the initial temperature is significant enough to interfere with the adsorption process.

B. Research Objective and Outline

This work first determines if there is a significant temperature change in the silica gel sample. Upon finding the temperature rise, the electrical heat effects and the adsorption heat effects are separated to determine the actual basis for the enhanced adsorption rates.

This report is organized in the following manner:
The theoretical basis for this study and the background
information are presented in Chapter 2. Chapter 3
describes the experimental arrangement and the experimental
procedure, Chapter 4 presents the experimental results,
Chapter 5 provides a discussion of the experimental results
and the conclusions and recommendations follow in Chapters
6 and 7 respectively.

Chapter II

Background and Theory

A. Heat of Adsorption

Depending on the types of bonds formed between adsorbate and adsorbent, adsorption can be described as physical or chemical. By definition, physical adsorption occurs when the adsorbate adheres to the surface by van der Waals forces (i.e. by dispersion or Coulombic forces). During the adsorption process, a quantity of heat is released known as the heat of adsorption. The heat of adsorption released during physical adsorption is approximately equal to the heat of condensation. Therefore physical adsorption is often described as a condensation process. Because the vapor pressure will increase with temperature, the amount of material physically adsorbed decreases as the adsorption temperature increases. The nature of the physical adsorption phenomenon is such that multiple layers of adsorbate will accumulate on the adsorbent surface.

Chemisorption is characterized by a sharing of electrons between the adsorbate and the adsorbent. The heat liberated during this process is approximately equal to the heat of reaction. Due to the sharing of surface electrons, chemisorbed materials are generally restricted

to a monolayer on the adsorbent surface. By definition, the thermal effects of physisorption and chemisorption appear quite different, but practically, a clear line of demarcation does not exist between the two mechanisms and both processes may occur simultaneously. (5)

The heat of adsorption depends on the adsorbateadsorbent system as well as the conditions under which the determination was made. Ross and Oliver have shown that the isosteric (constant adsorbate concentration) heat of adsorption may be expressed as (5):

$$\Delta H_{st} = RT^{2} \left(\frac{\partial \ln P}{\partial T} \right)_{e} = -R \left(\frac{\partial \ln P}{\partial \left(\frac{1}{T} \right)} \right)_{e}$$
(Eqn. 2.1)

 ΔH_{st} = Isosteric heat of adsorption

R = Gas Constant

T = Absolute temperature

P = Equilibrium pressure of the system

= Fraction of the surface covered by adsorbed molecules.

The heat of adsorption that is liberated when a solute is adsorbed on a surface will cause the temperature of the adsorbent to rise. The amount of heat liberated is directly proportional to the amount of material adsorbed, which is a function of the amount of solute in the influent stream and of the extent of saturation on the surface. The increase in bed temperature that might be expected due to

the heat liberated from the adsorption process is partially offset by heat transfer to the nonadsorbable carrier gas that flows through the bed. Since adsorption is an exothermic process, the concentration of adsorbed gas decreases with increased temperature at a given equilibrium pressure. (23) Thus, as the temperature increases, the adsorptive capacity of the solid adsorbent decreases. At higher bed temperatures, the equilibrium adsorption capacity of the adsorbent will be reduced and this will result in a shorter breakthrough time. (The breakthrough time refers to the length of time before a specified adsorbate effluent concentration is measured from an adsorbate-adsorbent system.) To determine breakthrough time, a fluid of adsorbate concentration Co is introduced to an adsorbent. The effluent adsorbate concentration is measured from an initial value of zero until some breakthrough concentration, Cb, is reached (corresponding to the breakthrough time). The appearance of Cb indicates that the adsorption rate is decreasing and a larger amount of adsorbate is exiting from the system. As bed temperatures increase and the adsorption capacity of the adsorbent decreases, the breakthrough concentration appears more quickly, thus resulting in a shorter breakthrough time for a given adsorbate-adsorbent system. (5)

Treybal (23) defines two heats of adsorption, differential and integral. The differential heat of adsorption $(-\overline{H})$ is defined as the heat liberated at

constant temperature when a unit quantity of adsorbate is adsorbed upon a large quantity of solid already containing adsorbate. A large or infinite quantity of solid is used to maintain a constant concentration of solid adsorbent. The differential heat of adsorption can be found from a plot of equilibrium adsorption pressure, $\overline{p}*$, versus the vapor pressure, p_v . The slope of an isostere (constant adsorbate concentration) is:

$$\frac{\mathrm{d}\ln\bar{p}^{*}}{\mathrm{d}\ln p_{*}} = \frac{(-\bar{H})_{M}}{\lambda_{r}M_{r}}$$
 (Eqn. 2.2)

 \bar{P}^{\bullet} = Equilibrium partial pressure of adsorbate

 p_{ν} = Vapor pressure of adsorbate

H = Differential heat of adsorption = Energy per mass of vapor adsorbed

 λ_{T} = Latent heat of vaporization of the reference substance at the same temperature

M = Molecular weight of the vapor being adsorbed

 M_r = Molecular weight of the reference substance.

The reference substance is a material (same as the adsorbable substance or different) at the same temperature as the adsorbate. Often, the reference substance is the pure substance being adsorbed, unless the temperature is above the critical temperature.

The integral heat of adsorption at any concentration

x of adsorbate upon the solid is defined as the enthalpy of the adsorbate-adsorbent combination minus the sum of the enthalpies of unit weight of pure solid adsorbent and sufficient pure adsorbate (before adsorption) to provide the required concentration x, all at the same temperature. If the differential heat of adsorption, \overline{H} , is computed at constant temperature for each isostere, the integral heat of adsorption at this temperature can be found from the following relation:

$$\Delta H'_{A} = \int_{0}^{x} H dx$$
 (Eqn 2.3)

- H' = Integral heat of adsorption = the energy per

 mass of the adsorbate-free solid, referred

 to the pure vapor
 - x = Adsorbate concentration, mass of adsorbate
 per mass of the solid.

Both the integral and differential heats of adsorption are functions of temperature and adsorbate concentrations for any system. (22)

B. Basis for this Work

Someshwar (20) performed studies concerning the electric field-induced effects on water vapor adsorption in porous adsorbents. Previous work offered only qualitative arguments to justify the speculation that adsorption rate enhancement in porous silica gel could be attributed to the additional electromagnetic forces on the polarized phases in the vapor adsorbate and adsorbent, resulting from the externally applied fields. Someshwar obtained quantitative estimates for the electromagnetic forces, ordinary concentration-gradient dependent forces and the rates of vapor adsorption in silica gel.

To compare the quantitative estimates of the polarized and charged-layer contributions to the overall mass flux, the following equation was used:

$$J_{\gamma_z} = -\lambda C_a \left[\left(\nabla \mu_{\gamma} \right)_z^{\circ} + \left(\nabla \mu_{\gamma} \right)_z^{\circ} + \left(\nabla \mu_{\gamma} \right)_z^{\circ} \right]$$
(Eqn 2.4)

J = Mass flux

 λ = A phenomenological coefficient

 C_d = Concentration of the diffusing species

 μ_{γ} = Chemical potential of the diffusing species Subsripts:

γ = Diffusing species

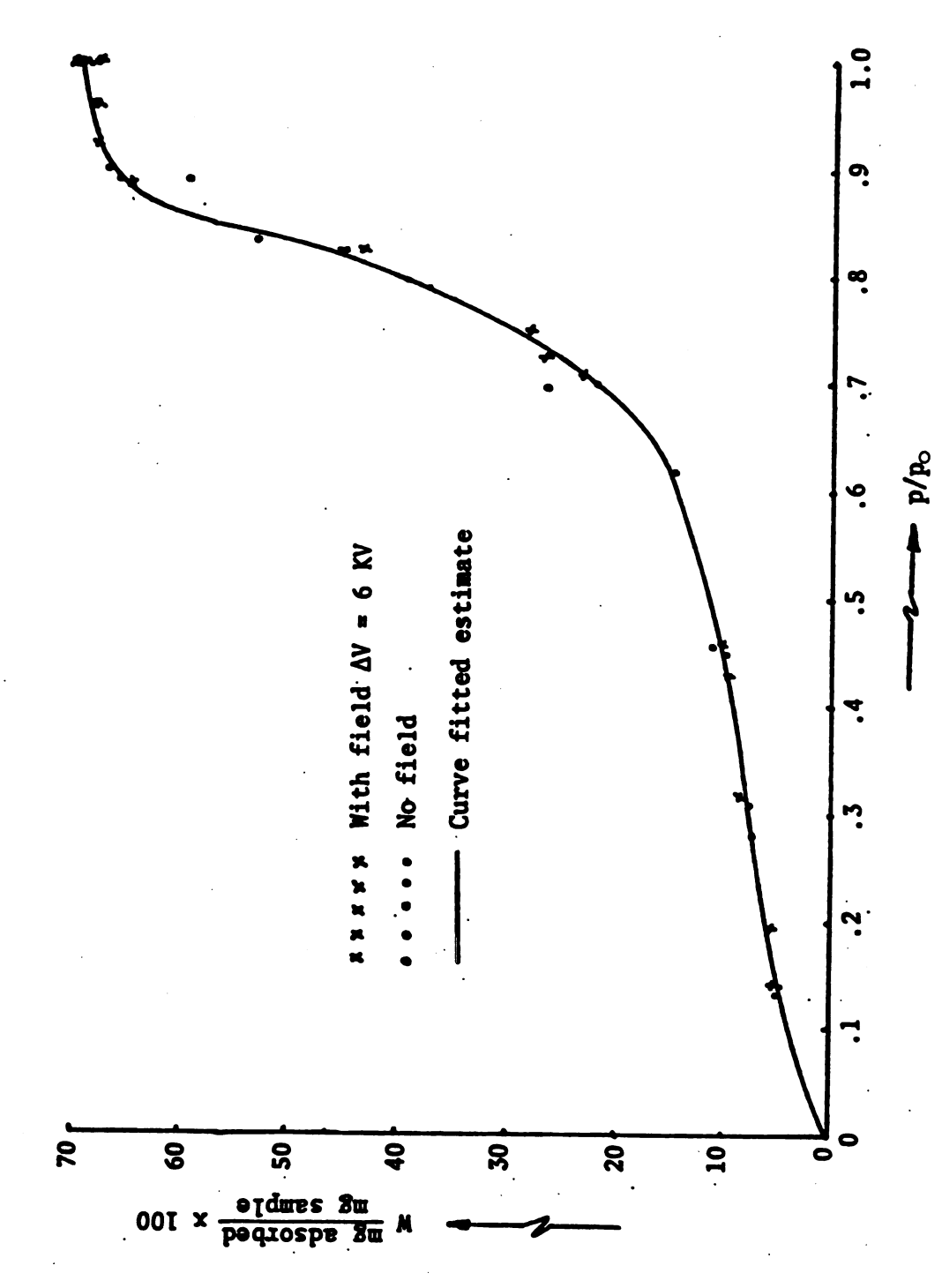
z = Direction of gradient

Superscripts:

- o = Value when the local electric field intensity is zero, V = 0.
- p = Polarized layer
- c = Charged layer

To overcome the geometric complexities of the silica gel, the sample was modeled on the basis of a single, open cylindrical pore with an average diameter of approximately 61.4 Å. The diffusion mechanism was assumed to be a combination of Knudsen and surface diffusion and a multilayer adsorption model described the process when the silica gel pores were subjected to a relative vapor pressure of $p/p_0 = 1$.

The material studied by Someshwar (20) was S-2509 Silica Gel manufactured by the Sigma Chemical Co. The adsorption isotherm for S-2509 Silica Gel is illustrated in Figure 2.1. The silica gel was subjected to DC electric fields of various magnitudes during water vapor adsorption to determine the field-induced effects on the water vapor adsorption process. The results of this work are shown in Figure 2.2. Adsorption rate enhancement occurred in the presence of a 6 kV externally applied DC electric field, during the multilayer adsorption phase of the process. Based on the assumption of isothermal conditions, the author concluded that the electromagnetic forces resulting



Adsorption Isotherm for Silica Gel S-2509; Amount Adsorbed (W) vs. Someshwar (20) Fraction of Total Saturation (p/p_0) ; T = 25 oC. Figure 2.1.

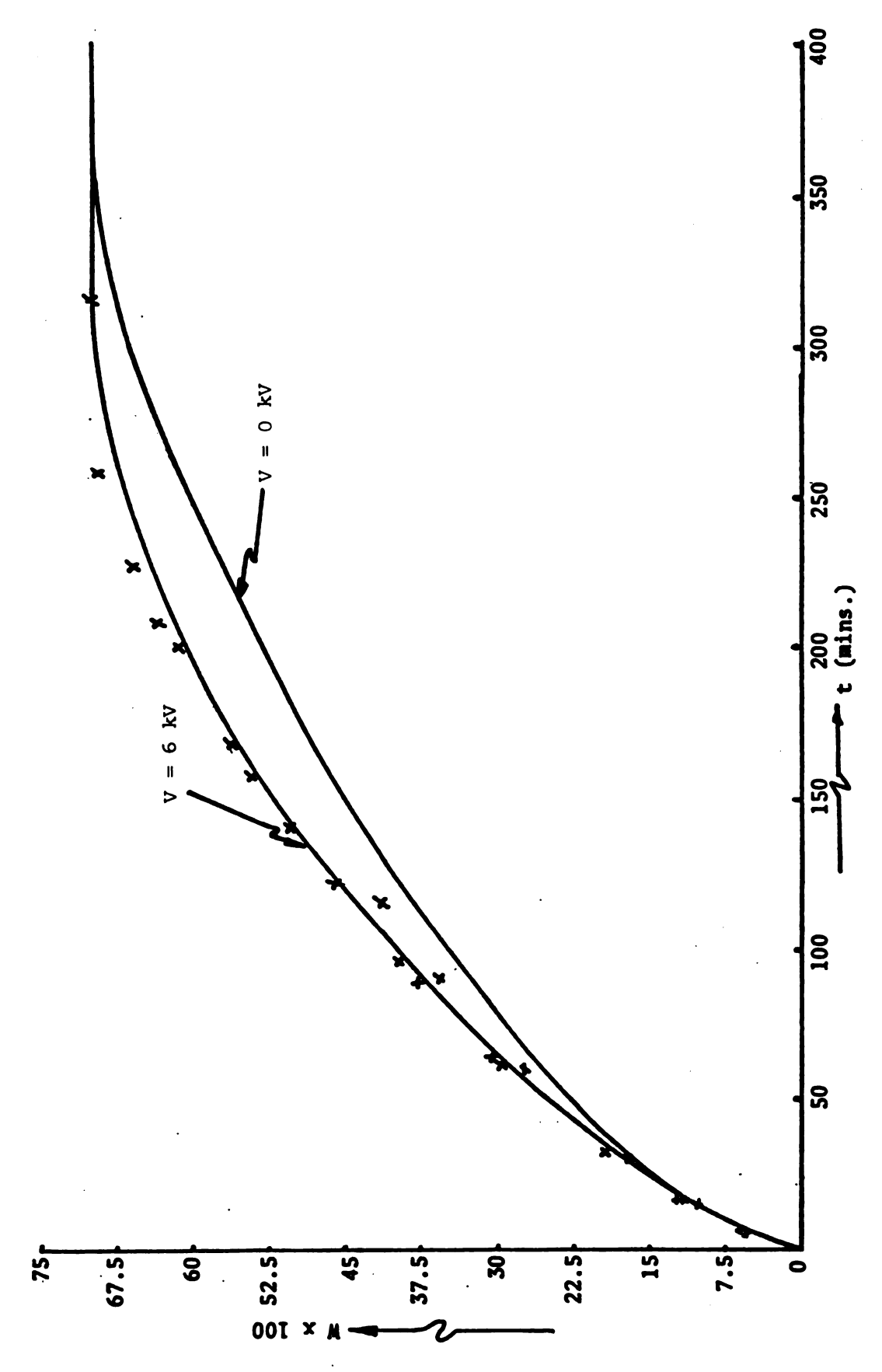


Figure 2.2. Adsorption of Water Vapor on Silica Gel S-2509 for V = 0 kV and V = 6 kV; p/p_0 = 0.9, T = 25 °C. Someshwar (20)

from the external field were responsible in total for the adsoption enhancement during the multilayer adsorption segment of the process. In the event that the assumption of isothermal process is invalid, it is unclear whether the adsorption enhancement is a result of the electric field or due to a temperature rise, generated by the presence of the electric field, which may increase adsorbate diffusion rates. If not addressed directly, increased diffusion rates will appear as increased adsorption rates. Similar results were obtained with 25 Å silica gel.

C. Current Research

1. Thermal Effects

Simultaneous measurements of diffusion and heat effects during sorption were performed by Kmiotek, Wu and Ma. (12) This study was performed to measure temperature rises during the sorption of methanol onto ZSM-5 Zeolite. Assuming isothermal conditions is not necessarily valid and, if significant thermal effects are present, both diffusion and adsorption can be affected. When large temperature rises are present, the use of isothermal models is not justified. If thermal effects are not considered, interpretation of diffusion data may lead to erroneous results.

The objective of the Kmiotek et al. work was to experimentally determine the temperature rise during adsorption and to ascertain the effects of these

temperature rises on the rate of adsorption. The results of this investigation indicate that the sorption curve is characterized by a very high initial adsorption rate followed by somewhat slower sorption. The temperature history curve is characterized by a rapid temperature rise followed by slow radiative cooling, indicating a maximum temperature rise of nearly 50 °C at approximately t=10 minutes. The rapid temperature rise is the result of the high initial adsorption rate. The high temperature rises occurred on freshly activated samples, lower temperature rises were found for subsequent adsorption on regenerated samples.

The maximum temperature rise can be correlated as a function of one of the dimensionless parameters characterizing the adsorbate-adsorbent system. The maximum temperature rise was found to follow the relation:

$$\frac{(\Delta T)_{max}}{T_{o}} = b \left(\frac{(\Delta H) M_{o}}{M_{o} C_{p} T_{o}}\right)^{1.05}$$
(Eqn. 2.5)

b = Function of the sample size

T = Temperature

 T_{\circ} = Initial temperature

H = Heat of adsorption

 M_{\circ} = Initial solute in the solid

 M_{\bullet} = Final solute in the solid

C_p = Heat capacity of solid.

At low total pressures, radiation is the primary means of heat transfer. As the total pressure approaches the vapor pressure, convective heat transfer becomes significant.

Kmiotek et al. concluded that large temperature rises may be experienced during adsorption if heats of adsorption are high and if heat transfer is slow compared to mass transfer. The initial heating is approximately adiabatic and the authors felt that the steep temperature rise results in a more rapid adsorption rate. The maximum temperature rise can be correlated as a function of the ratio of the total heat generated during sorption to the heat capacity of the zeolite. No attempt was made to quantitatively predict the diffusion coefficient and activation energy due to the large number of parameters involved. In summary, the authors concluded that the use of isothermal models for the determination of diffusion coefficients appears to be inappropriate when large temperature rises occur.

Kmiotek et al. felt that adsorption rate increased as temperature increased and therefore they imply difussion enhancement. As previously mentioned, they did not quantitatively predict a corrected diffusion coefficient and appear to employ this implication without fully substantiating it. Within the parameters of this study, adsorption enhancement resulting from temperature rise appears plausible. The authors state that the temperature rise is the result of the high initial sorption rate and

that this temperature rise increases the sorption rate, producing a net large temperature rise in a short period of time. However, this is in disagreement with the majority of existing knowledge indicating that adsorption rate decreases as system temperature increases. For example, as the temperature increases, the vapor pressure of the gaseous adsorbate will increase, thus decreasing the driving force for adsorption. Therefore, while the temperature rise data during the adsorption experiment has merit, the contention that adsorption rate increases with temperature appears questionable.

Lee and Cummings (14) observed the adsorption of water onto silica gel to seek correlations between the analytical solution for isothermal conditions and nonisothermal experimental data. Temperature rises of up to 100 OF (38 OC) were observed in industrial gas driers resulting from the heat of adsorption. The investigators found that the bed temperature rise causes a decrease in capacity and also gives distorted breakthrough curves as compared with isothermal conditions. In general, the rate of mass transfer in water vapor adsorption by silica gel adsorbent is controlled by the diffusion through the gas film surrounding each desiccant particle. Therefore, gas phase mass transfer control was assumed by Lee and Cummings in performing this research. This mass transfer limitation on adsorption indicates that any electric field effect acts on the gas phase.

Lee and Cummings (14), found that the lower adsorption capacity of desiccants in nonisothermal dynamic operations as compared with isothermal operations is primarily due to the rise in bed temperature during the drying operation. The principal heat source is the heat of adsorption, with the dry air acting as a coolant, resulting in bed temperature rises proportional to the fraction of water vapor in the gas phase and inversely proportional to the fraction of dry air in the gas phase. If the absolute humidity of the influent is very low, the heat effect will be very small and the isothermal condition is approached. Therefore, as the absolute humidity of the influent approaches zero, the nonisothermal breaktime approaches the isothermal breaktime.

2. Adsorption Rate Enhancement Using Electric Fields
The surface interactions of a fluid and a solid can
be affected through the application of an electric field.
Lincoln and Olinger (16) found that the adsorption rate of
ethylene onto nickel was increased in the presence of a
4 kV AC voltage, while the adsorption rate of hydrogen onto
the same surface was unaffected by the electric field.
Isosteric heats of adsorption computed from ethylene
isotherms ranged from 2200 to 1700 calories per gram mole
for the 0.0 kV data and from 7500 to 5000 calories per gram
mole for the 4.0 kV data. Lincoln and Olinger (16) felt
this difference in the heats of adsorption to be

significant and indicative of a possible shift in the mechanism of adsorption.

Lincoln and Olinger (16) felt that the results of their study indicate that adsorption rate and quantity can be inceased for some gases through the use of a high potential. They felt that their work provides evidence that these changes are centered more in the chemical than the physical aspects of adsorption and supported this conclusion by citing the following two results: (1) a shift in the heat of adsorption and the adsorption mechanism accompanies the altered adsorption rates, and (2) as adsorbate diffusion becomes important at higher pressures, the effects of the imposed voltage on adsorption diminish.

Many heterogeneous catalysis reaction rates have recently been increased using electric fields. Keier, Mikheeva and Usol'tseva (10) enhanced the dehydration of isopropyl alcohol on TiO₂ films by the presence of a 6.5 kV fixed electric field. A reduction in the activation energy for the reaction was also found while using the electric field. Dere'n and Mania (3) investigated the effect of an electric field on the oxidation kinetics of CO to CO₂ on a ZnO surface. A sharp increase in the reaction rate was found for electric fields of -4 kV DC. The magnitude of the effect increases with increases in the field and with decreases in temperature. The interesting feature of this study is that the reaction rate returns, after a certain time, to the initial value in spite of the

continuing field presence. The duration of this effect is from 5 to 25 minutes. Dere n and Mania (2) also found reaction enhancement for CO oxidation on nickel oxide. The presence of the DC electric field (of positive polarization) induces a positive space charge in the closeto-surface layer of NiO, thus accelerating the catalytic process. The effect observed becomes larger as the electric field intensity is increased. Based on their experimental research and Wolkenstein's electronic theory of catalysis and chemisorption on semiconductors, Dere'n et al. generalized that since catalytic reaction involves chemisorption of the reacting gases on the catalyst surface (as one of the elementary steps), it can be expected that an electric field should also affect catalytic activity. An electric field influences the chemisorptive properties and some catalytic processes of a number of semiconductors.

Additional study of carbon monoxide oxidation on nickel oxide catalyst was performed by Lee (15) using an A.C. field of 22,000 volts per centimeter intensity (peak to peak) and various frequencies. This investigation concluded that the oxidation rate was a function of field frequency and that the maximum rate of oxidation occurred between 100 and 200 cycles per second. Lee, in collaboration with Hsu (8), performed additional A.C. field studies on the hydrogenation of benzene to cyclohexane using nickel and brass catalysts. The final conclusion of this work states that the electrodynamic field effect

exists in semiconductor catalysis, as well as in a metal catalyst, for the oxidation and hydrogenation reactions tested.

D. Energy Balance

An unsteady-state energy balance is used to describe the thermal effects of the adsorption process in the presence of an electric field. Appendix A provides the details of the energy balance derivation. It is assumed that the free adsorbate and carrier gas stream does not appreciably increase in temperature. Calculations (see Appendix C) indicate that the maximum possible rise in the gas stream temperature is 0.082 °C (0.148 °F). The removal of heat from the silica gel occurs due to convective heat transfer with the gas stream flowing through the adsorption chamber. Therefore the $\mathring{m}_{air}^{C}_{pair} \Delta T_{air}$ term is considered negligible.

This energy balance on the silica gel sample yields:

$$m_{sg}C_{psg}\frac{dT_{sg}}{dt} = \dot{m}_{ads}\Delta H_{ads} + 0.0569IV - UA\Delta T_{sga} \qquad (Eqn. 2.6)$$
$$-3.968 \times 10^{-3} \dot{m}_{aix}C_{paix}\Delta T_{aix}$$

 m_{sg} = Mass of the silica gel sample (mg)

 C_{psq} = Specific heat of silica gel (Btu/mg-OF)

 T_{SG} = Temperature of the silica gel (OF)

t = Time (min)

m
ads = Adsorption rate of water onto silica
gel (mg/min)

 H_{ads} = Heat of adsorption (Btu/mg)

I = Electric field current (Amperes)

V = Electric field potential (Volts)

 \dot{m}_{air} = Mass flowrate of moist air (mg/min)

Cpair = Specific heat of moist air (Btu/mg-OC)

 $T_{air} = Temperature of moist air (<math>^{\circ}C$)

U = Overall heat transfer coefficient
(Btu/min-ft²-OF)

A = Area for heat transfer (ft^2)

 T_{Sga} = Temperature difference between the silica gel and the moist air. (OF)

Initial Condition:

 $T_{SQ} = T_{SQO}$

Physical Constants:

$$C_{psg} = 0.22 \text{ Btu/lb-OF}$$
 (18)

$$\Delta H_{ads} = 16.0 \text{ cal/gm}$$
 (17)

The silica gel temperature changes can be predicted by rearranging and approximating the above differential equation to:

$$\Delta T_{sq} = \frac{\left(\dot{m}_{ads} \Delta H_{ads} + 0.0569 IV - UA\Delta T_{sqa}\right) \Delta t}{m_{sq} C_{peq}}$$
(Eqn 2.7)

The numerical value of the UA combination used in the above energy balance was determined from the experimental data. For several time intervals the temperature change of the silica gel was combined with the calculated theoretical temperature rise derived from the heat of adsorption at the given adsorption rate. From this information, a heat load was determined and from the calculated temperature change the UA term could be found using $q = UA \triangle T$. See Appendix B for an example of the above calculations.

E. Relaxation Field Discussion

The electric fields producing the effect on the water vapor adsorption are, in general, not uniform. The local fields depend on both the overall field and the local environment. A brief discussion of this phenomenon follows.

Due to the cylindrical pore shape in silica gel and the long narrow pore structure, the adsorption of water on silica gel is generally represented by a diffusion-controlled mass transfer mechanism.

As adsorption is occurring, the regions close to the pore mouths tend to have a greater concentration of adsorbate than those deep in the center. Due to the differing dielectric constants associated with monolayer adsorbate, bound layer adsorbate, condensed layer adsorbate and vapor phase adsorbate, the local electric fields will vary along the pore. Generally, the fields at the pore

mouth will be smaller, due to higher dielectric constants, than the fields at the pore center. (20) This will create a field gradient toward the center of the pore. This field and the corresponding electric field will vary continuously with the adsorption process. Someshwar (20) felt that the fields in the pore would relax as the process of adsorption continued. He felt that although these internal field gradients produced by relaxation depend on the overall magnitude of the externally applied electric field, they are much larger in magnitude than the macroscopic field gradients in the bulk adsorbent sample.

Chapter III

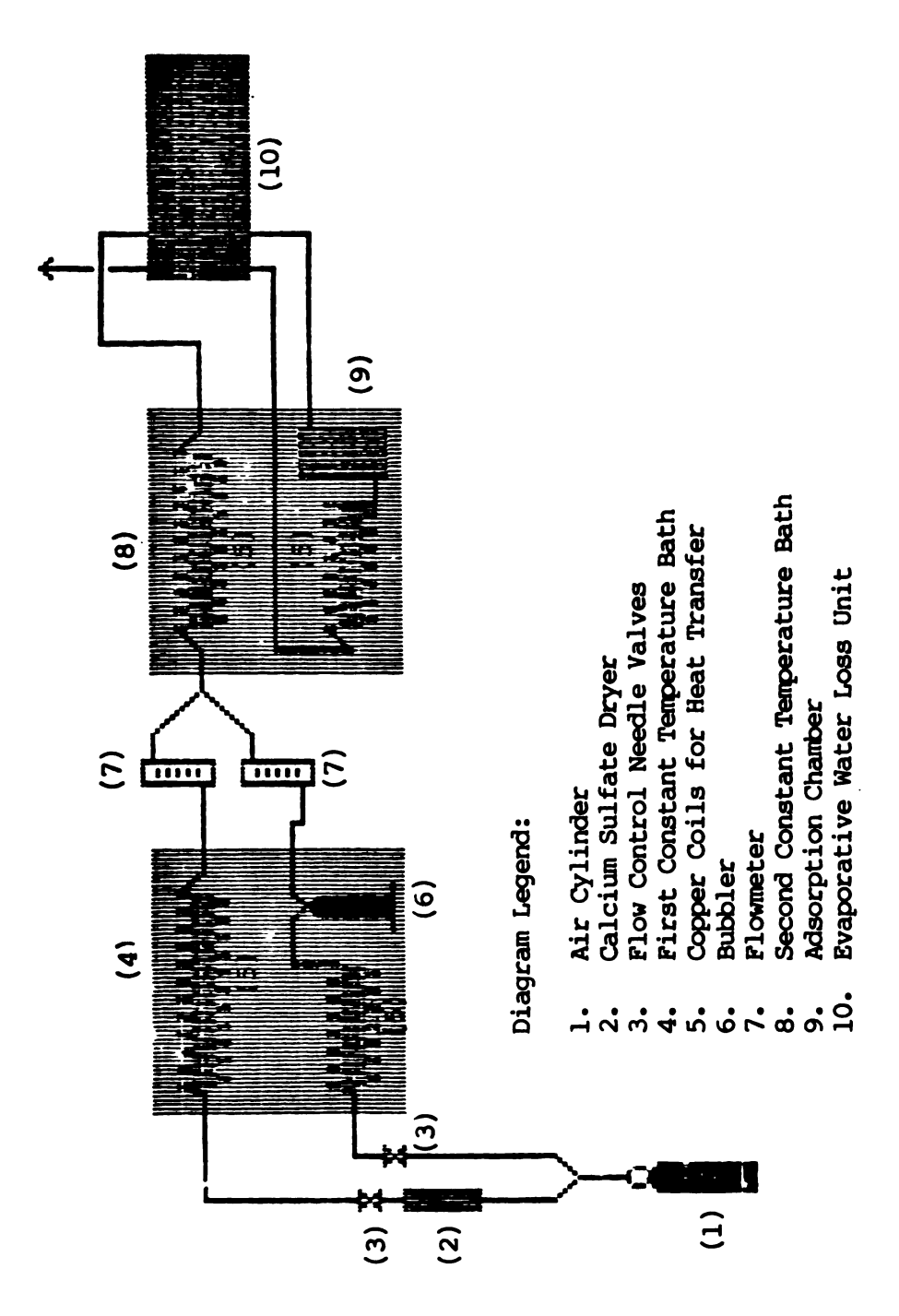
Experimental Equipment and Experimental Procedure

In an effort to reduce measurement errors, indirect methods of data acquisition have been integrated into the experimental portion of this thesis. In particular, adsorption rates are measured by observing changes in the water content of the gas streams rather than by directly weighing the silica gel samples. This provided instantaneous adsorption rate information and did not require the removal of the external potential during adsorption rate data acquisition. This chapter of the thesis will first describe the flow scheme for the adsorption experiments and provide detailed discussions of individual pieces of equipment as required. Following the flow scheme description, the electric field generation will be discussed. This included the integration of a thermocouple into the silica gel to determine temperature changes. Next, the equipment used for data acquisition will be described and the chapter will conclude by outlining the experimental procedure.

A. Description of the Flow Scheme

A schematic diagram of the experimental flow arrangement is in Figure 3.1. The flow originates at the pressurized air cylinder. The gas flow (at 8 psig) passes through a calcium sulfate dryer and is immediately split into a dry stream and a stream to be saturated with water vapor in the first of two constant temperature baths. Both the wet and dry streams pass through copper coils submerged in the first constant temperature bath (maintained at 25 °C) to ensure an equal and constant gas temperature. Following the copper coil, the damp stream passes through two distilled water bubblers, also submerged in the first bath, to saturate the gas stream with distilled water at 25 °C and approximately 4 psig. Following the first constant temperature bath, both the wet and dry air streams pass through needle valves, used to control the flowrates, and Lab-Crest Century flowmeters, used to monitor the flowrates. Following the flowmeters, the wet and dry streams are combined to achieve a stream with the desired fraction of full saturation. The humidity of the resulting stream is controlled by the flowrates of the wet and dry streams used to form the combined stream. This stream then flows through a copper coil in the second constant temperature bath to return it to 25 °C.

Following the first copper coil in the second bath, the gas stream, with previously determined humidity, flows into the Evaporative Water Loss Unit (EWLU). The EWLU uses

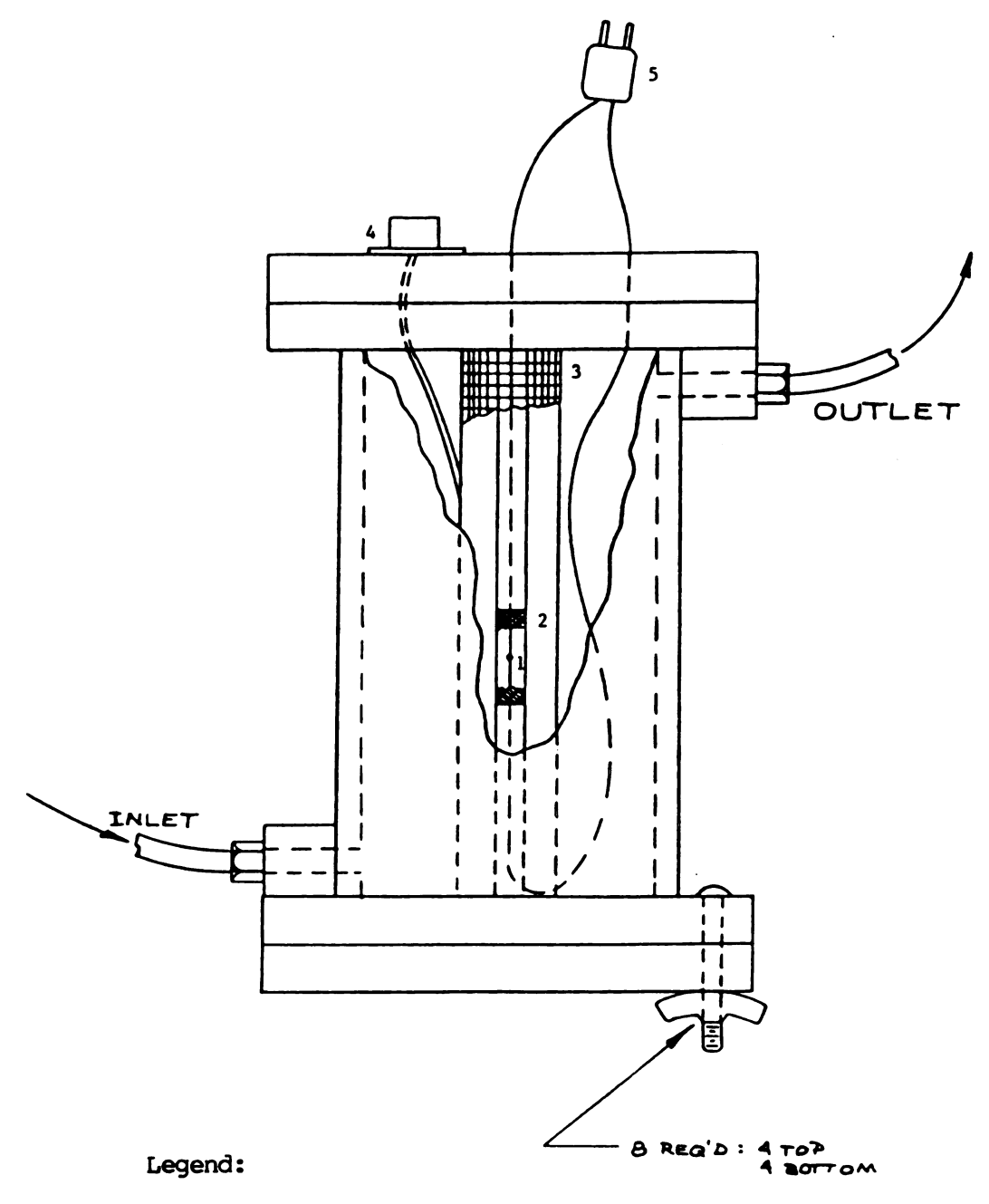


Schematic Diagram of Experimental Flow Arrangement. Figure 3.1.

two matched thermistors to compare the thermal conductivity (and, hence the vapor content) of the gas stream before and after it passes by the adsorbent sample. The details of the EWLU will be discussed in Section B of this chapter. The stream with the known humidity is used as the reference stream for the EWLU, passing over one of the two thermistors. This stream exits the EWLU, flows through a second copper coil submerged in the second constant temperature bath and then flows to the adsorption chamber (also submerged in the second bath) containing the silica gel sample. The adsorption chamber is a plexiglass cylinder four inches long and two and one half inches in diameter, as shown in Figure 3.2. The silica gel sample is centered axially in the adsorption chamber and surrounded by an electrode. A detailed description of the adsorption chamber is found in Section B of this chapter. The gas stream leaves the adsorption chamber and passes across the second thermistor of the EWLU to determine changes in its vapor content due to adsorption. The EWLU produces a voltage proportional to the difference in thermal conductivity of the two streams. The gas stream leaves the EWLU as system effluent.

For experiments in which only temperature

measurements were taken, the EWLU was removed from the flow
scheme. In these instances the gas stream formed by mixing
the dry and wet streams will flow directly into the
adsorption chamber, pass over the silica gel sample and



- 1. Thermocouple junction, also functions as the negative electrode of the electric field.
- 2. Section containing silica gel sample.
- 3. Positive electrode of the electric field.
- 4. Coaxial connector for the electric field.
- 5. Thermocouple connector to cold junction compensator.

Figure 3.2. The Adsorption Chamber

exit the adsorption chamber as system effluent.

B. Detailed Equipment Descriptions

1. Evaporative Water Loss Unit (Demco Model Z-1334)

The EWLU is a device employing a thermal conductivity cell and an electrical bridge circuit to determine the difference in thermal conductivity of two gas streams. The instrument was developed by Dr. Thomas Adams (1) of the Michigan State University Physiology Department and produced by Demco Research and Development of Lansing, Michigan.

The EWLU continuously and simultaneously compares the thermal conductivity of two air streams. One stream has a known water vapor content and the other stream has a different and varying vapor content. The sensing unit and its thermally regulated enclosure are constructed so the temperature, flowrate and distribution of the air streams is always the same across the two thermistors, which are the basic detection elements. See Figure 3.3 for a schematic representation of the EWLU.

Moist air, of a chosen and constant humidity, flows from the compressed air source, through the bubblers and to the EWLU. Inside the EWLU, this air passes through a heat exchanger to regulate its temperature at approximately 50 $^{\circ}$ C, flows over a reference thermistor (T_{mr}) and out of the EWLU into the adsorption chamber. Water vapor is removed from the flow stream and the drier air flows back

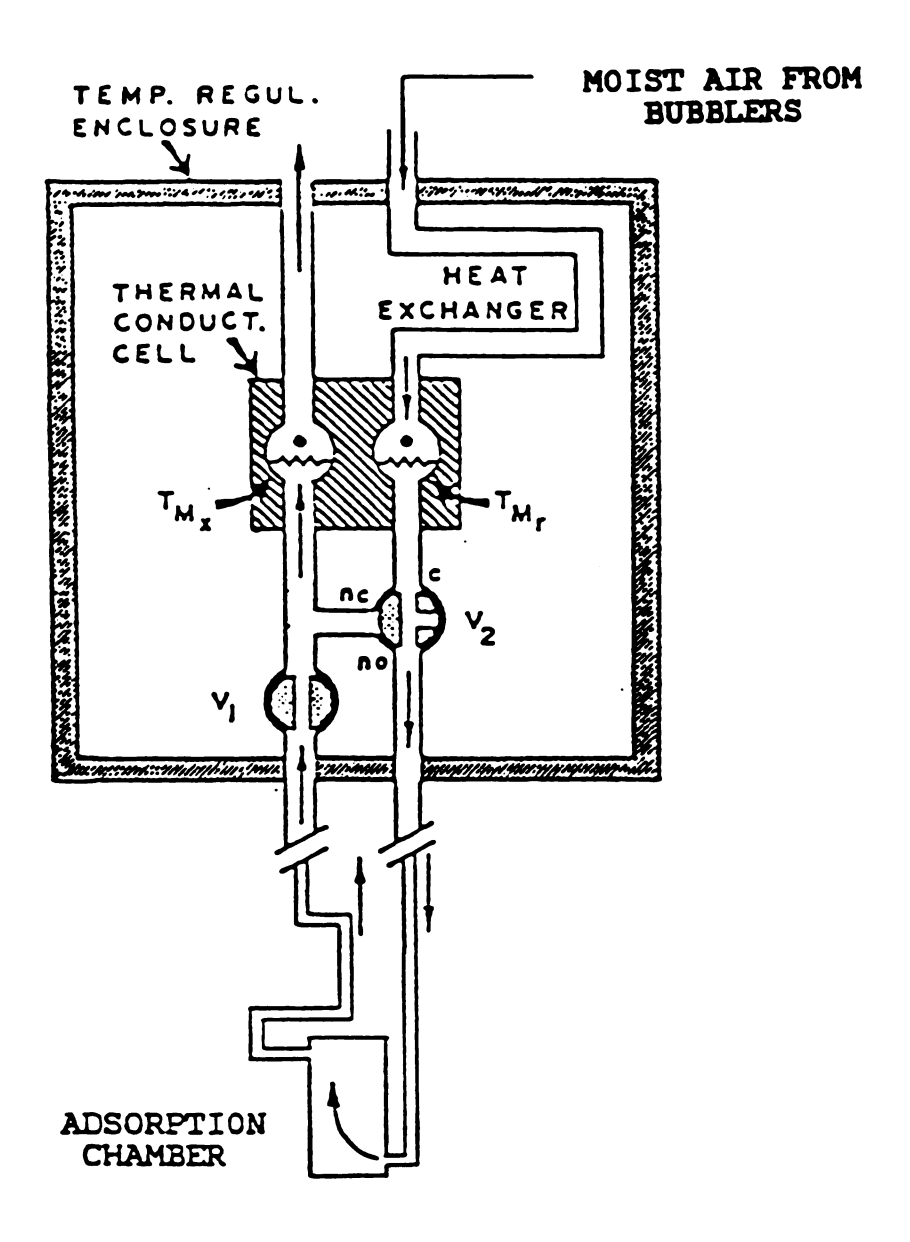


Figure 3.3. Function of the Evaporative Water Loss Unit.

The moist air from the bubblers passes through a heat exchanger within a regulated (nom. 50 °C) enclosure at a nominal rate of 200 cc/min before flowing over the reference thermistor, Tmr. The damp stream then flows over the silica gel sample, in the adsorption chamber, and across the matched thermistor, Tmx, mounted in the sample side of the thermal conductivity cell. The sample is then vented to the atmosphere. Valves (Vl and V2) control the path of the air stream so that it either flows directly from the reference to the sample side of the cell, for balancing the voltage divider, or through the adsorption chamber for a measurement. This sketch is not drawn to scale. Adams et al. (1)

into the EWLU, passing over the matched thermistor (T_{mx}) mounted in the sample side of the thermal conductivity cell before it is vented to the room air. The two thermistor beads $(T_{mr}$ and $T_{mx})$ are two of the four legs of a resistance bridge. To "zero" the bridge, both thermistors are exposed to the reference (moist) air stream by shunting the adsorption chamber with valves V_1 and V_2 . When the voltage divider has been balanced, the flow can be passed through the adsorption chamber and adsorption measurements taken.

Calibration of the EWLU was performed by injecting accurately known volumes of water into a test cell and determining the signal corresponding to the evaporation rates so produced. These data were then plotted and fit to a straight line. The analog output voltage of the EWLU is calibrated as a linear function of water adsorbed or water evaporated in milligrams per minute. The calibration curve generated prior to performing these experiments can be found in Figure 3.4.

The EWLU was designed to measure water evaporation from sufaces. Therefore, its normal operation uses a dry reference stream which passes through a test cell picking up evaporating moisture. To accommodate the experimental arrangement for this work, the reference stream is the "moist" air stream, created by the valving and bubblers prior to the EWLU. The unknown stream follows the adsorption cell and therefore contains less moisture than

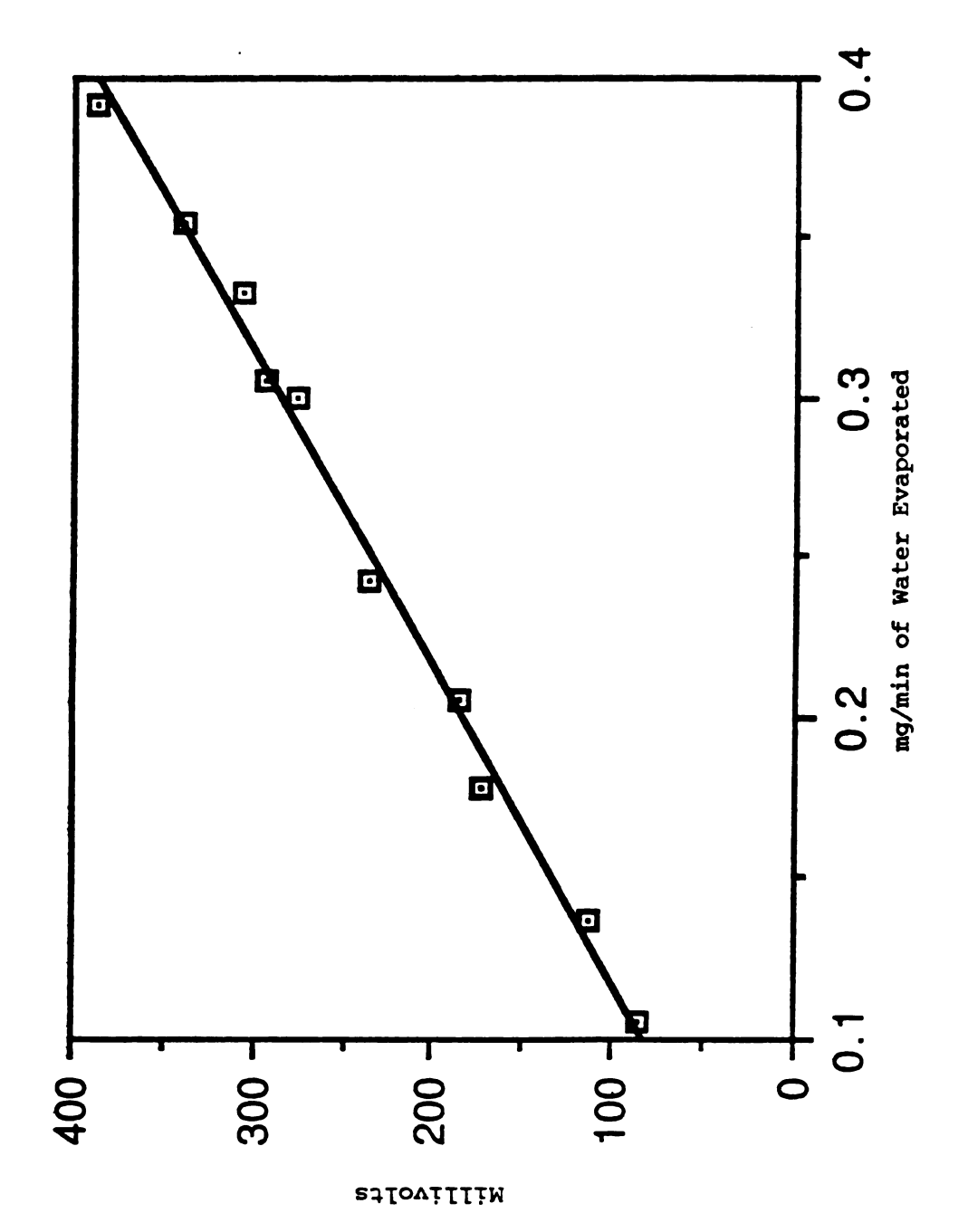


Figure 3.4. Evaporative Water Loss Unit Calibration Curve.

the reference stream.

2. The Adsorption Chamber

The adsorption test cell is an airtight plexiglass cylinder with an inlet for moist air flow and an outlet for air that has passed over the silica gel sample. The cylinder is flanged on each end to accommodate the flat, plexiglass bottom and top, which are held in place by bolts and wing nuts. The top is fabricated with openings to accommodate the entrance and exit of thermocouple leads used to monitor the temperature of the silica gel sample. These leads also serve as electrical ground for the electric field. The top also contains a coaxial connector to input the positive electrode of the electric field to the cell (see Figure 3.2).

The electric field is produced by charging a copper mesh screen of 2.5 centimeters diameter, installed concentrically to the sample inside the plexiglass cell. The silica gel sample is placed concentrically inside the copper screen. The sample is held in a screen cylinder 0.35 centimeters in diameter with a length of approximately 1.3 centimeters. The electric field ground wire is inserted longitudinally. The mass of the silica gel sample is 50 to 60 milligrams.

For temperature monitoring, the junction of an iron/constantan thermocouple is located at the center of the silica gel sample and acts as a ground wire. The wire

is grounded when the electric field is being applied to the sample and passes through a Simpson 269 Series 3 Ultra High Sensitivity Volt Ohm Microammeter for field current monitoring. To monitor the sample temperature, the field is turned off and the silica gel temperature is determined using a Honeywell Potentiometer, Model 2720 in conjunction with an Omega Engineering thermocouple cold-junction compensator, Model Omega CJ-J. The temperature can then be found from millivoltage reference tables. A digital multimeter was also used to determine thermocouple output, and provided identical values as the Simpson 269.

The D.C. electric field, employed for adsorption enhancement experiments, is created by connecting a Spellman High Voltage D.C. Power Supply to the coaxial connector on the adsorption chamber top.

C. Data Acquisition

1. Adsorption Data

As mentioned previously, the output of the EWLU is an analog voltage in the millivolt range. Calibration of the EWLU provided a correlation between the rate of adsorption in milligrams of water adsorbed per minute and the EWLU output voltage. The collection and storage of this information was performed using an IBM XT personal computer. Interfacing with the IBM XT was achieved using a Data Translation Brand analog to digital (A/D) converter, Model DT2805.

The data translation equipment was calibrated to accurately read EWLU output voltages from 0 volts to 1.0 volts within approximately .05 millivolts. This is sufficient to record the adsorption data, but does not provide the accuracy required to record the silica gel temperature.

2. Temperature Data

The temperature of the silica gel sample was monitored using an iron/constantan (type J) thermocouple. The diameter of this thermocouple was chosen as 0.005 inches because the thermocouple wire also functioned as the ground potential conductor for the external electric field. The small diameter wire maximizes the variation in electric field within the sample. The thermocouple wire passes axially along the center of the adsorption chamber and places the joint of the dissimilar iron and constantan leads halfway along the axial length of the silica gel sample. The thermocouple bead is formed by bringing the iron lead in through the top of the cell, twisting it to the constantan lead and soldering the connection. The twisting is done in an end to end fashion to ensure that the thermocouple wire functions as a single wire passing axially through the cell (and axially through the silica gel sample) when the external electric field is applied.

The temperature readings are taken by determining the millivolt output of the thermocouple and employing

thermocouple temperature-millivolt reference tables. To avoid the problems and inaccuracies associated with maintaining an ice bath thermocouple reference, a cold junction compensator from Omega Engineering, Model CJ-J, is employed. The cold junction compensator provides a steady electrical thermocouple reference corresponding to zero degrees Celcius and outputs an accurate thermocouple signal on copper leads to be read by a potentiometric device.

3. Use of Data

The adsorption data, milligrams of water adsorbed per minute, is taken in through the Data Translation A/D board and and analyzed by the IBM XT. This information represents the rate of instantaneous adsorption at the time the data was taken. The rate data, in millivolts, is converted to milligrams of water per minute by software in the IBM XT. The program was conceived and written by Gregory Stevens.(22) The conversion is carried out using the calibration equation for the EWLU. The total amount of water adsorbed by the silica gel is found by numerically integrating the instantaneous rate data over time using a trapezoidal rule. To normalize the results for comparative purposes, the total amount of water adsorbed is reported by the program as milligrams of water adsorbed per milligram of silica gel sample.

37

D. Experimental Procedure

There are two procedures required to perform the experiments outlined in this work. Procedure Number One describes the experimental method for determining temperature changes in the silica gel and Procedure Number Two describes the method for determining adsorption rates in the presence of an external electric field. The General Procedure reports the steps common to the preparation required for both types of experiments.

1. General Procedure

Prior to the Start of All Experiments

- a. The silica gel is prepared for experimental analysis by drying overnight in an oven at 130 °C. It is removed from the oven, placed in a desiccator and allowed to cool to room temperature.
- b. Both constant temperature baths are brought to 25 °C using Haake temperature controllers.

2. Procedure Number One

Temperature Experiments

- a. The thermocouple wire is threaded loosely through the adsorption chamber and centered in the silica gel sample screen.
- b. The sample screen is filled with dryed, room temperature silica gel.
- c. The dry air flow is started to fill the experimental

- flow system with dry air and create a slight positive pressure in the adsorption chamber for sample loading.
- d. The sample cell is placed in the adsorption chamber and the thermocouple wire is pulled taut to ensure that it will pass axially through the cell and the silica gel sample.
- e. The adsorption chamber is sealed and placed in the second constant temperature bath. The coaxial cable for electric field creation is connected for field experiments.
- f. The thermocouple connections are made and the silica gel and water bath temperatures are monitored until they equilibrate.
- g. The equilibrated temperature is recorded as the temperature at time = 0 and the damp air flow is started and adjusted to the specified value. The electric field is applied for field experiments.
- h. At five minute intervals, the electric field is turned off and the temperature is recorded.

3. Procedure Number Two Adsorption Measurements

- a. The adsorption chamber, not containing any silica gel, is connected to the EWLU, placed in the second temperature bath and allowed to equilibrate with its surroundings.
- b. Moist air, of the saturation to be used for the

experiment, is passed through the empty adsorption chamber until the output of the EWLU remains a constant voltage. This indicates all adsorption on the experimental equipment is complete and therefore will not compromise the silica gel adsorption data.

- c. The bridge of the EWLU is then balanced to give an output of 0.0 millivolts.
- d. The silica gel sample is loaded into the sample screen and placed in the adsorption chamber.
- e. The data acquisition program is started and run until adsorption is completed.
- f. At the end of the experiment, the data is integrated numerically to determine the total amount of water adsorbed.

Chapter IV

Experimental Results

The purpose of this section of the thesis is to present the experimental results of this investigation. The initial experiments were performed to establish the existence of a substantial rise in temperature during the adsorption process. This rise in temperature was measured as a function of time with p/p_0 equal to 0.7, 0.8 and 0.9 at 25 °C. (The fraction of total water saturation in the gas stream is defined as p/po.) An air stream saturated with water would be mixed with a dry air stream to form a given water vapor concentration. These experiments were performed in the presence of a highly non-uniform 6 kV DC electric field as well as in the absence of an electric The temperature history profiles were examined in conjunction with the prevailing knowledge of adsorption phenomena to deduce conclusions from these results. should be noted that the above p/p values are correct as stated. The Evaporative Water Loss Unit (EWLU) was not employed during the temperature studies. It was found to interfere with the gas stream saturation values and will be discussed later in Chapter 4 and in Chapter 5.

The most significant point of each temperature history curve is the maximum temperature experienced by the silica gel and its corresponding time of occurrence. These

values approximate the initial adiabatic temperature rise due to the heat of adsorption for water onto silica gel. Section A will present the results of the experiments which did not employ an electric field; Section B will present the results of experiments in the presence of a 6 kV electric field and Section C will compare and contrast the two above cases. All experiments were performed at 25°C in an air/water flow system of 200 cubic centimeters per minute.

A. Experiments in the Absence of an Electric Field on S-2509 Silica Gel

The temperature history curves for the non-field experiments (V = 0 kV) on S-2509 Silica Gel, manufactured by the Sigma Chemical Company, exhibit a rapid initial temperature rise followed by an approximately exponential temperature decay. The properties of S-2509 Silica Gel can be found in Table 4.1.

Table 4.1.

Properties of S-2509 Silica Gel (20)

Source: Sigma Chemical Company

Size Range: 63-210 Am

Mean Pore Radius: 30.7 Å; Bulk Density: 0.461 g/cm²

Specific Surface Area: 456.1 m²/g of dry adsorbent

Total Void Fraction: 0.794; Internal Void Fraction: 0.323

Monolayer Adsorbed Water: 0.0649 mg/mg of dry adsorbent

The temperature change of the silica gel is reported as the increase in the temperature from time equal to zero, i.e., the beginning of each experiment. Experiments were begun following equilibration of the silica gel temperature with the bath temperature. Table 4.2 gives the maximum temperature increase of the silica gel and the approximate time of its occurrence for the experimental values of p/p_0 . In all of the non-field experiments, the time of maximum silica gel temperature increase varied between t=10 minutes and t=15 minutes, depending on the time required for the gas flows to be adjusted. As each experimental trial began, it was necessary to adjust the wet and dry flows to obtain the proper gas stream saturation.

Table 4.2.

Maximum Silica Gel Temperature Increase

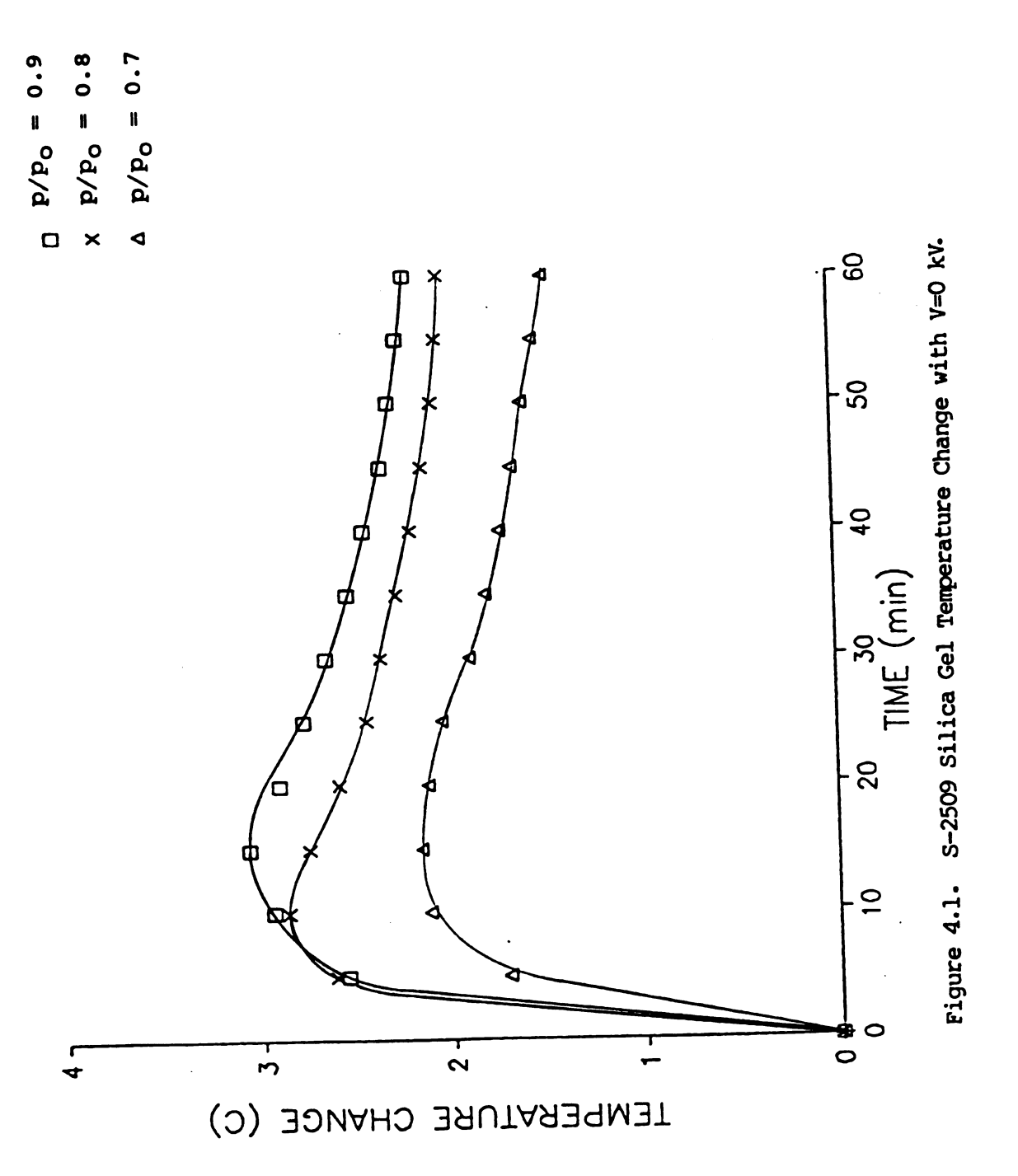
(V = 0 kV)

		Approximate Time of <u>\(\Delta T \text{max} \) (min)</u>	
p/p _o	ΔTmax (^O C)		
0.9	3.1	13	
0.8	2.9	12	
0.7	2.2	12	

Adjustment of the flow greatly affects the experimental data. Any flow adjustment during the experiment appeared

immediately in the temperature data, causing a deviation from the normal smooth curve of the silica gel temperature versus time profile. As a result, flow misadjustment at the beginning of an experimental trial or an extended flow adjustment period at the beginning of an experimental trial, caused the maximum silica gel temperature occurrence to vary slightly from one run to another. Careful study of several experimental runs produced an average value of the time to attain the maximum temperature increase. average value is reported in Table 4.2 (See Appendix F for raw data). The maximum temperature increase occurs at approximately t = 13 minutes for $p/p_0 = 0.9$ and at approximately t = 12 minutes for $p/p_0 = 0.7$ and 0.8. difference in time of the occurrence of the maximum temperature can be explained by the differing adsorption rates. As the concentration of water increases, the adsorption rate and the total amount adsorbed increase. a result, the adsorption rate is initially less in the lower concentration ranges and is less throughout the experiment. Therefore, the maximum temperature is lower and occurs earlier in the experiment for the lower p/p values.

Figure 4.1 displays the temperature history profiles for the first hour of experimental time at $p/p_0 = 0.7$, 0.8 and 0.9 in the absence of an electric field. (See Appendix F for raw data.) As indicated by both Table 4.2 and Figure 4.1, the maximum silica gel temperature increases as



the adsorbate concentration of the influent gas increases. Following the attainment of the maximum silica gel temperature, the temperature history curves for all adsorbate concentrations show an exponential decrease in silica gel temperature. This steady drop in temperature occurs throughout the portion of the adsorption experiment following the maximum silica gel temperature, until the silica gel temperature reaches the water bath temperature. This steady reduction in temperature occurs for several reasons. First, the adsorption rate steadily decreases as the experimental time increases, thus generating less heat due to adsorption. Second, convective heat transfer continues to occur and therefore the experimental gas stream is continuously carrying heat away until the gas temperature reaches the bath temperature.

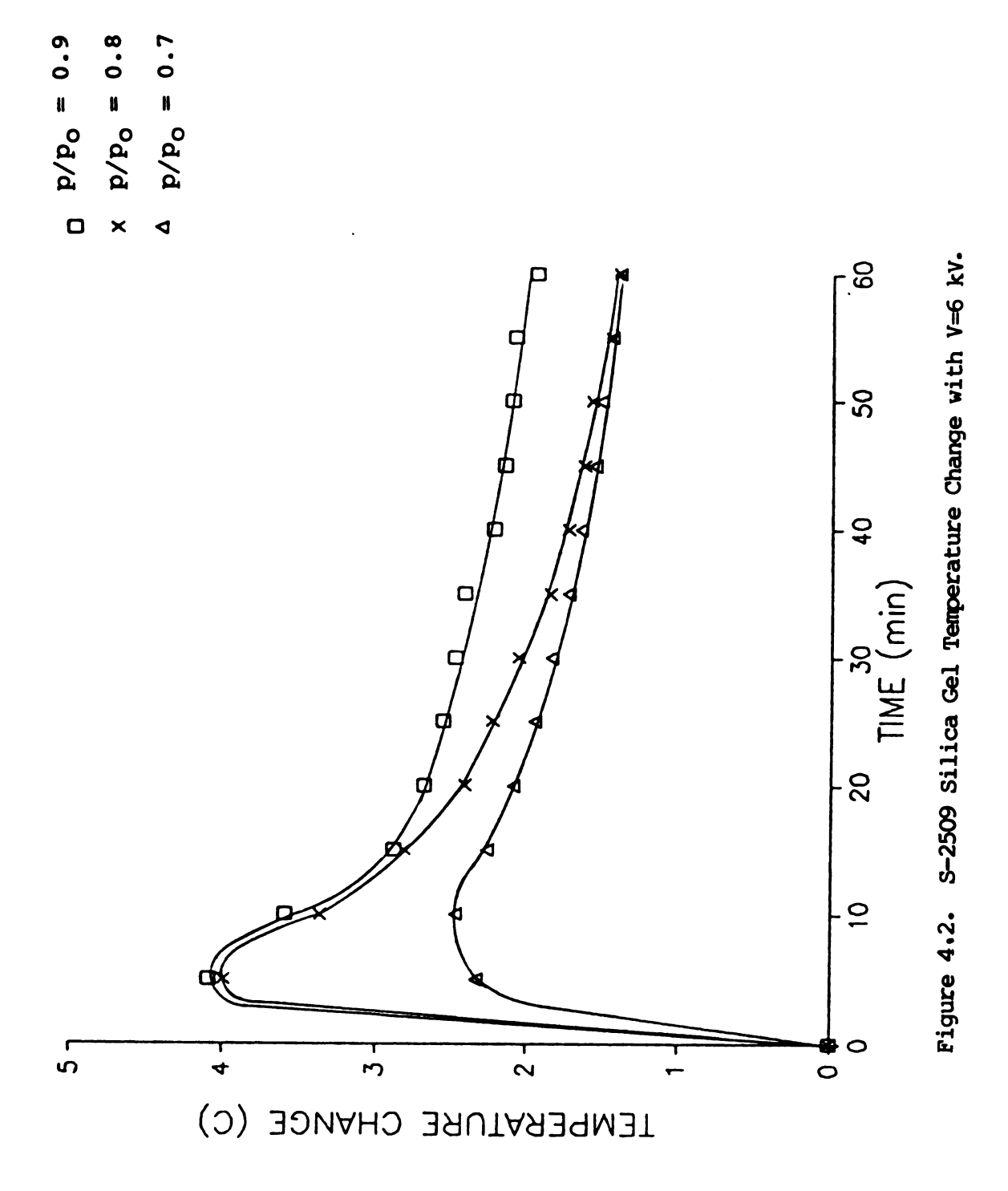
B. Experiments in the Presence of an Electric Field on S-2509 Silica Gel

The temperature history curves which indicate water vapor adsorption enhancement on S-2509 Silica Gel are for experiments performed in the presence of a 6 kV DC electric field. Field currents were monitored and determined to be in the 1 to 10 nanoampere range. In the presence of a 6 kV DC electric field with $p/p_0 = 0.9$, the field current was 6 nanoamperes during the first five minutes of each experiment and increased as the experiment continued. Field currents were 4 to 5 nanoamperes for $p/p_0 = 0.8$ and 1

to 2 nanoamperes for $p/p_0 = 0.7$ in the first five minutes. The results of the field experiments are qualitatively similar to the non-field results, but differ quantitatively. Both field and non-field experiments exhibit a sharp initial rise in the temperature of the silica gel, followed by an exponential decrease in the sample temperature. Although the general trends of the temperature data are similar, the initial rise in silica gel temperature in the presence of an electric field is more rapid and of greater magnitude as compared to data generated in the absence of an electric field. temperature history curves for experiments in the presence of a 6 kV DC cylindrical highly non-uniform electric field are shown in Figure 4.2 for $p/p_0 = 0.7$, 0.8 and 0.9 respectively. (See Appendix F for raw data.) Table 4.3 contains the significant information for adsorption experiments in the presence of a 6 kV non-uniform DC electric field.

Table 4.3. Maximum Silica Gel Temperature Increase (V = 6 kV)

		Approximate Time	
p/p _o	ΔT _{max} (^O C)	of ΔT_{max} (min)	
0.9	4.1	5	
0.8	4.0	5	
0.7	2.5	10	



In the presence of the 6 kV DC electric field, the maximum temperature increase of the silica gel is still a function of the adsorbate concentration, however the difference of the maximum temperatures obtained between $p/p_0 = 0.8$ and 0.9 is less than the temperature difference realized in the absence of an electric field. In addition, the maximum temperature rise in the presence of a 6 kV electric field occurs earlier (at t = 5 minutes, for $p/p_{O} = 0.8$ and 0.9, as compared to 12 to 13 minutes in the V = 0 kV case). Following the attainment of maximum temperature rise, the temperature difference from initial silica gel temperature exhibits the expected exponential reduction found in previous experiments. The maximum temperature rise of the silica gel sample at $p/p_0 = 0.7$ is not nearly as prompt as the result at higher adsorbate concentrations and therefore more closely resembles the nonfield data at this adsorbate concentration.

C. Comparison of Field and Non-Field Experimental Results

The comparison of the silica gel temperature rise in
the presence and absence of an applied electric field will
be employed here to begin forming the basis of the
conclusions established from this investigation. Table 4.4
summarizes Tables 4.2 and 4.3 in order to facilitate
comparison of the two experimental arrangements.

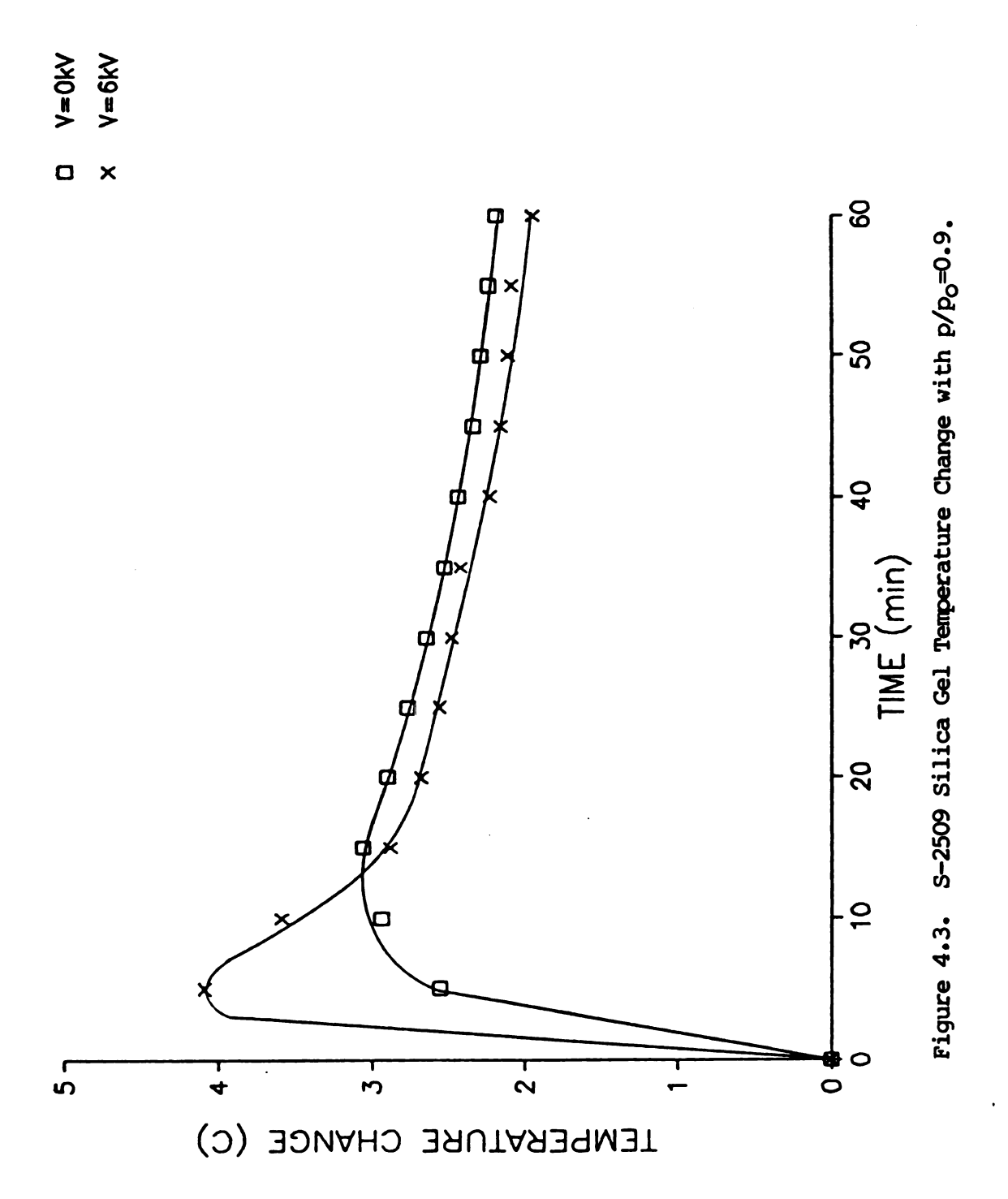
Table 4.4.

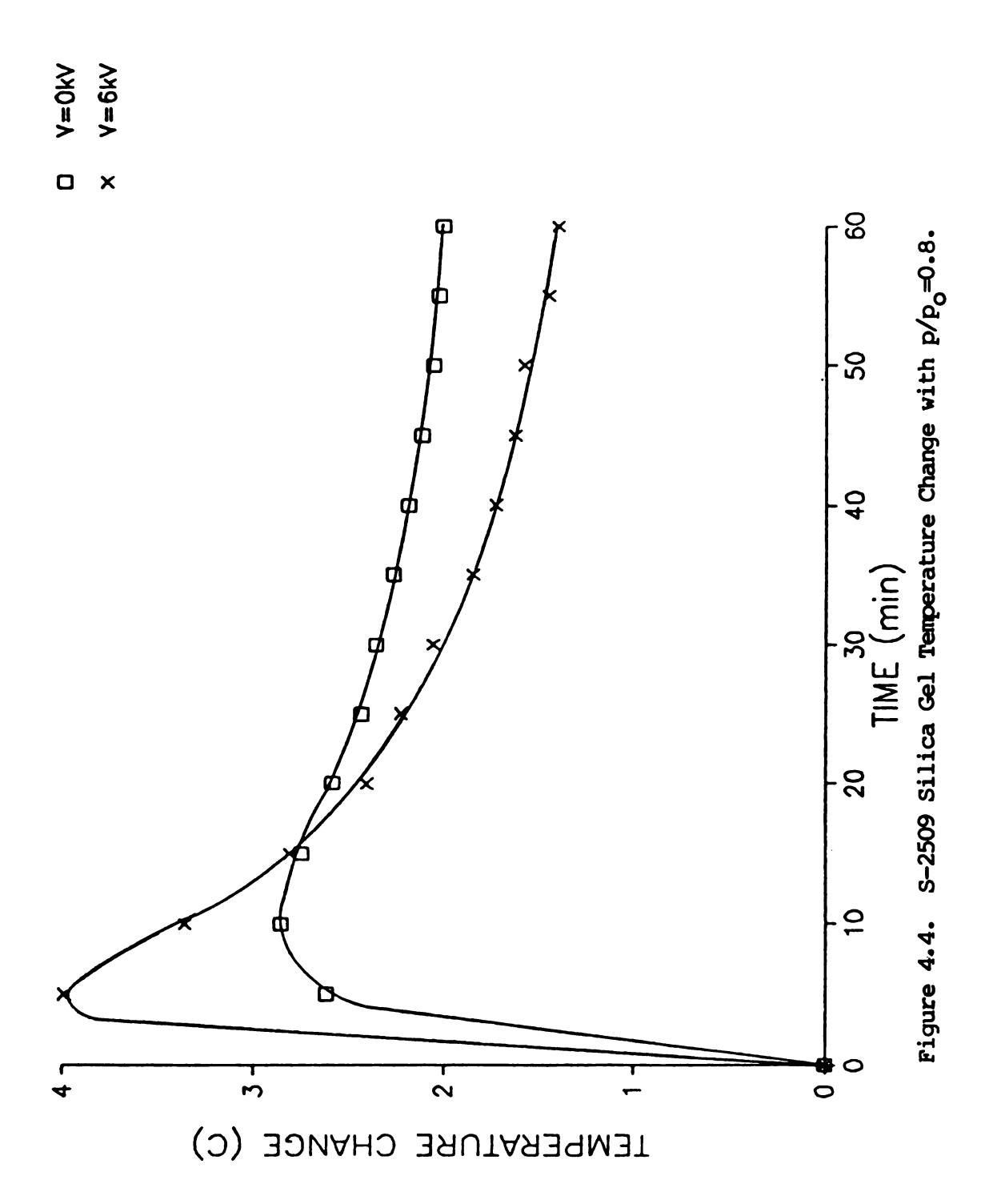
Maximum Silica Gel Temperature Increase

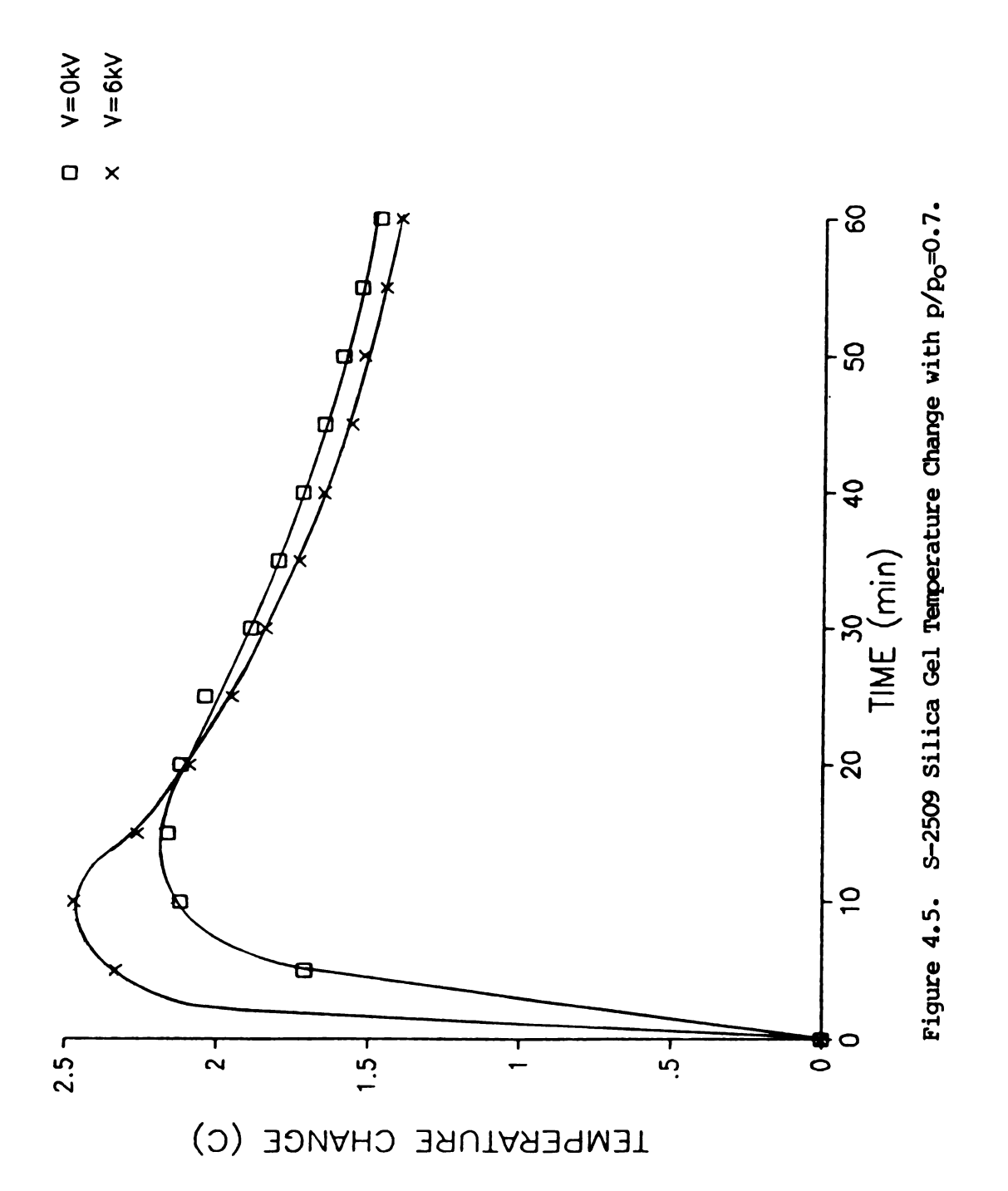
			Approximate Time
p/p _o	<u>V (kV)</u>	ΔT_{max} (°C)	of ΔT_{max} (min)
0.9	0	3.1	13
0.9	6	4.1	5
0.8	0	2.9	12
0.8	6	4.0	5
0.7	0	2.2	12
0.7	6	2.5	10

Figures 4.3, 4.4 and 4.5 will graphically compare the field and the non-field data for $p/p_0 = 0.9$, 0.8 and 0.7 respectively.

Comparison of the field and non-field experimental results reveals general trends in the thermal behavior of the S-2509 Silica Gel during the adsorption process. The maximum silica gel temperature rise occurs earlier and is of greater magnitude in the presence of a 6 kV electric field than in the absence of the electric field at $p/p_0 = 0.7$, 0.8, 0.9. Following the maximum silica gel temperature rise, all of the temperature history curves exhibit an exponential decrease in silica gel temperature







due to convective heat transfer.

Examination of the data for $p/p_0 = 0.8$ and 0.9 shows a marked difference in the results obtained at V = 0 kV and V = 6 kV. In the presence of a 6 kV electric field, both of the aforementioned adsorbate concentrations exhibited maximum temperature increases of similar magnitude occurring at approximately t = 5 minutes. The non-field results show the maximum temperature rises occurring between t = 10 minutes and t = 15 minutes. Also, the temperature rise at each water vapor concentration is of smaller magnitude than the corresponding value at V = 6 kV and the magnitude of the temperature rise is a direct function of the gas phase adsorbate concentration. The differences in the temperature profiles at V = 0 kV and V = 6 kV indicate an increased adsorption rate in the presence of an electric field of 6 kV.

The maximum silica gel temperature increase for the $p/p_0 = 0.7$ occurs at t = 10 minutes in the presence of a 6 kV electric field as compared to approximately t = 12 minutes for V = 0 kV. In addition, the magnitude of the temperature increase is only slightly larger in the presence of the electric field than otherwise. The temperature history curves are very similar in shape and magnitude for $p/p_0 = 0.7$, in contrast to the differing shapes of the field and non-field curves for $p/p_0 = 0.8$ and 0.9.

During the phase of the experimentation concerning

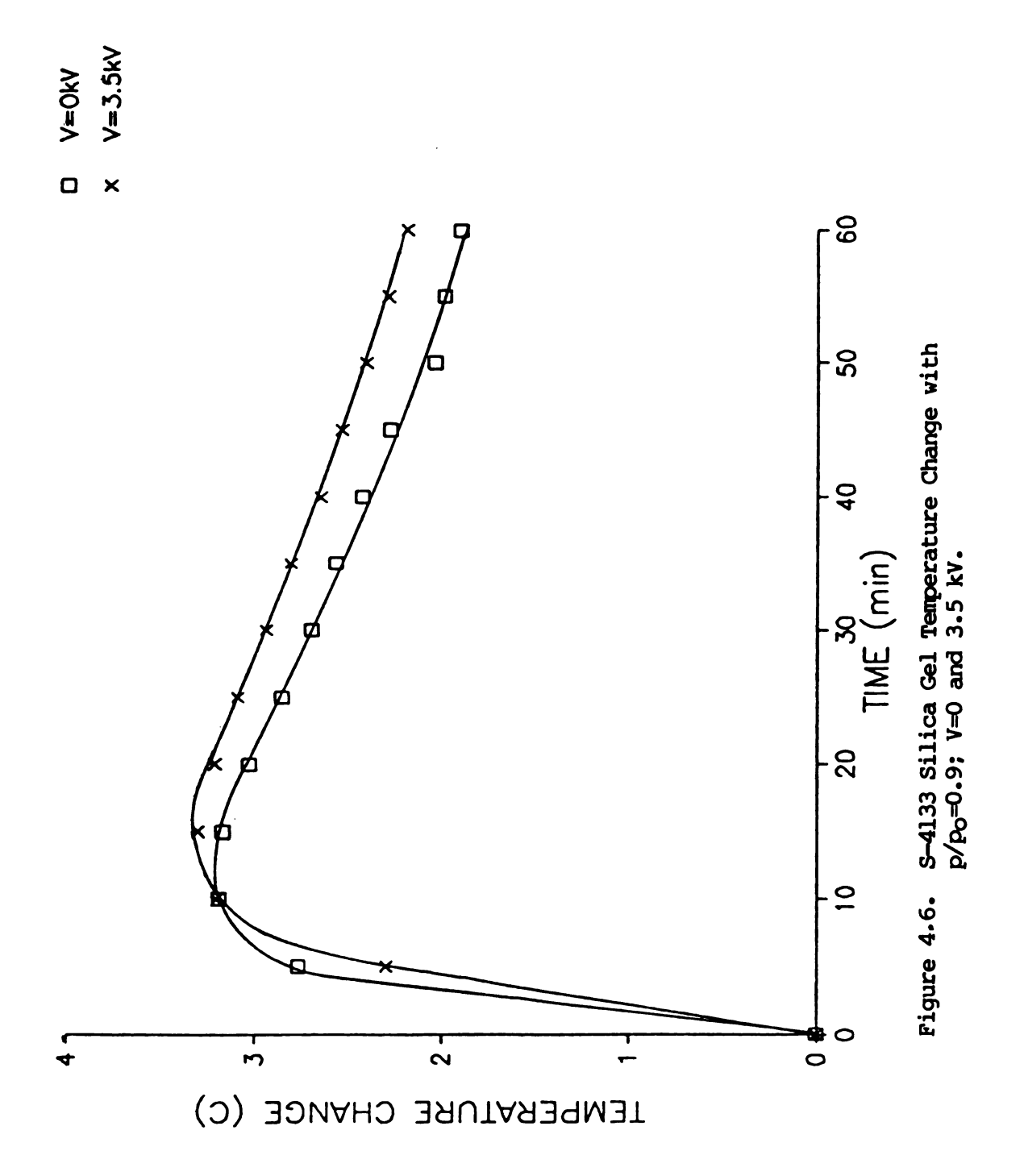
 $p/p_0 = 0.7$ with V = 6 kV, the maximum silica gel temperature fluctuated from one experimental run to another. (See Appendix F for raw data.) Consequently, as maximum temperatures varied, the remaining experimental temperatures varied. It was found that small errors in adjusting the moist air and dry air flowrates for $p/p_0 = 0.7$ resulted in large fluctuations in the maximum temperature rise of the silica gel. For example, if the moist air flowrate were to be set approximately 7% high $(p/p_0 = 0.75$ as compared to 0.70), the experimental data would approximate the data expected at $p/p_0 = 0.8$ with V = 6 kV.

Additional experimentation was performed on the silica gel in order to determine the affect of the DC electric field on the silica gel temperature. The temperature of the silica gel was monitored with the electric field applied and dry air, from the calcium sulfate dryer, flowing over the silica gel. Therefore, no adsorption would be occurring and only the DC electric field would cause temperature increases. The results of this work showed silica gel temperature increases no greater than 0.08 °C. Calculations in Appendix E predict a maximum temperature rise of 0.039 °C/min with a 6 nanoampere field current, as measured during the first five minutes of an experiment. Over a five minute period, this contributes 0.195 °C of adiabatic temperature rise resulting directly from the 6 kV DC electric field. This

indicates that the rise in temperature is due primarily to the heat generated by the adsorption process. The application of the field alone does contribute to the silica gel temperature rise. However, only a small portion of the temperature rise is due to the electric field, as compared to the adsorption related temperature rise. The temperature rise may also be due in part to changes in the heat of adsorption of the adsorbate-adsorbent system in the presence of an electric field as found by Lincoln and olinger. (16)

D. Experiments on S-4133 Silica Gel

Preliminary experiments for this thesis work were performed on S-4133 Silica Gel, mean pore diameter of 25 A, from the Sigma Chemical Company. The temperature of the silica gel was monitored throughout the water vapor adsorption process while subjected to a 3.5 kV electric field and without the application of a field, both at $p/p_0 = 0.9$. The temperature history curves exhibit virtually identical behavior in either instance. Figure 4.6 compares the field and non-field cases. Data taken for the duration of the adsorption process, showed the silica gel temperature returning to its original value after four to five hours of experimentation. The nearly equal maximum temperatures for the field and non-field cases indicates no adsorption enhancement is occurring and actually shows a decrease in the initial adsorption rate



when V = 3.5 kV. The slight and constant difference in the field and non-field temperatures shows heating due to current flow.

It must be noted that the adsorption rates found during this work were taken following the completion of the temperature studies due to malfunctions of the Evaporative Water Loss Unit (EWLU). These equipment problems were comprised of a drift in the datum voltage for the EWLU and, although they were less pronounced during the adsorption rate determination portion of this investigation, their continued occurrence compromised the adsorption rate data. Secondly, following the completion of both the temperature and adsorption rate studies, the pressure drop across the EWLU was found to be approximately 9 psi. This flow stream expansion significantly reduced the saturation level of the experimental gas stream. Based on the water content in air at the experimental temperature and pressure, (19) a stream of $p/p_0 = 0.9$ at 2 atmospheres would be approximately $p/p_0 = 0.42$ after expanding across the EWLU. This stream would further expand to $p/p_0 = 0.23$ at 1 atmosphere. (See calculations in Appendix D.) Therefore, the adsorption rate data was not included with the temperature data, because the two types of experiments (including the EWLU and excluding the EWLU) represented different gas stream saturation levels. As a result, the adsorption rate data found with the EWLU should be considered as secondary to the temperature work and only as supportive of the trends

found in this investigation. The adsortion rates increased as the gas stream saturation levels increased, thus supporting the trend of higher temperature rises in the silica gel with increased stream saturation levels.

Chapter V

Discussion of Experimental Results

The purpose of this section of the thesis is to address the experimental results which require clarification or comparison with previously established information, to provide insight into any discrepancies in the results and to determine the causes for any deviations from previous of expected results. Employing the information from the aforementioned comparisons, the basis for the conclusions drawn from this work will be formed.

A. Discussion of Results for S-2509 Silica Gel

The temperature profiles for $p/p_0 = 0.8$ and 0.9 indicate immediate adsorption enhancement in the presence of an electric field. The abrupt rise in temperature in the presence of the 6 kV electric field is the result of increased adsorption rates. Someshwar (20) concluded that adsorption rates were not influenced by the electric field during the formation of the first few layers of adsorbate on the silica gel surface, which occurred during the first 20 minutes of experimental time. Throughout most of this study, the adsorption rates, found from the EWLU, were thought to be lower than those reported by Someshwar (20). This led to speculation that the silica gel was not being

properly dried and thus contained a monolayer of water prior to the start of experimentation. However, continued experiments to determine the total amount of water adsorbed were performed. By weighing the silica gel following drying, subjecting it to the moist gas stream in the experimental cell for periods from four hours to 12 hours and then weighing the silica gel again, the total amount of water adsorbed at saturation could be determined. agreed very well with Someshwar's results. As final verfication, the damp silica gel would then be dried and weighed. The weighings of the dried silica gel substantiated that all of the adsorbed water was removed during our drying process. This proved that the silica gel was not contaminated with an existing layer of water prior to experimentation. The final explanation for the apparently low adsorption rates, found in this work relative to those in the Someshwar work, was determined to be caused by the EWLU. Following the experimental portion of this work, it was determined that the EWLU contributed a significant pressure drop within the system. The measured pressure drop of 9 psi reduced the p/p value from 0.9 to 0.42 (see Appendix D for supporting calculations). Therefore, when the EWLU was added to the flow scheme to determine the adsorption rates, the rates were less than anticipated. The temperature studies in this thesis were performed in the absence of the EWLU and therefore duplicate the Someshwar work. The temperature rise might

be explained by a change in the heat of adsorption, based on a change in the adsorption mechanism, in the presence of an electric field (however, see discussion below).

Although the field geometry and the adsorption sample cell employed in this work duplicated the Someshwar arrangement as nearly as possible, small unknown nuances in the experimental details could have contributed to the discrepancies discussed above.

The abrupt heating of the silica gel sample due to the heat of adsorption from the initially high adsorption rate indicates that the silica gel sample does not rapidly exchange heat with its environment. This is also apparent from the small value of UA determined for the system $(UA = 1.31 \times 10^{-4} \text{ Btu/hr-}^{\circ}\text{F}, \text{ see Appendix B})$. As the adsorption rate continues to decrease, the generation of heat lessens and the energy stored in the silica gel is removed through convective heat transfer with the carrier gas. In addition, the sudden silica gel temperature increase indicates the possibility of an increase in the heat of adsorption in the presence of a 6 kV electric field, however, this change in heat of adsorption is unlikely. Figures 4.3, 4.4 and 4.5 indicate that after the initial temperature rise of the silica gel in the presence of an electric field, the temperature actually falls below the temperature of the non-field case as the experiment Therefore, additional heat is not being generated by an increased heat of adsorption.

Significant adsorption enhancement was realized immediately for $p/p_0 = 0.8$ and 0.9 in the presence of a 6 kV electric field. The temperature history curves and the adsorption rate data are very similar between the $p/p_0 = 0.9$ and 0.8 cases. The similarity between the maximum temperature obtained at $p/p_0 = 0.9$ and $p/p_0 = 0.8$ and the similarity in the time that they occurred strongly indicate that the rates of adsorption are initially very similar when the adsorption rate is increased by an electric field. However, the adsorption isotherm (20) (Figure 2.1) for water vapor adsorption onto silica gel indicates that the adsorption amount in milligrams of adsorbate per milligrams of adsorbent is less at $p/p_0 = 0.8$ than at $p/p_0 = 0.9$. Also, the indication from this temperature study and numerous adsorption studies firmly illustrate that the rate of adsorption is a direct function of the adsorbate concentration in the influent gas. Therefore, it was difficult to justify, on the basis of only the temperature study, that the initial adsorption rates for the $p/p_0 = 0.9$ and 0.8 cases were identical, due to the different water vapor concentrations. Originally the EWLU was to be employed to confirm this result, however, initial adsorption rates were unable to be determined using the EWLU.

Someshwar (20) found adsorption enhancement was delayed until approximately 20 minutes into each silica gel adsortion experiment, coinciding with the completion of the

bound monolayer. The electric field enhancement therefore, occurred during the multilayer adsorption phase. Isothermal conditions were assumed throughout his work. Therefore, it is possible that if the application of the electric field caused an unusual rise in the temperature of the silica gel, the diffusion rate may have been improved, thus resulting in an apparent adsorption rate increase. At t = 25 minutes during the temperature studies, the temperature of the silica gel subjected to an electric field is actually less (0.1 °C) than silica gel not subjected to an electric field. Because of this contradiction between the Someshwar work and this temperature study, calculations (see Appendix E) were performed to predict the effect on the silica gel temperature produced by the field current measured during the experimental portion of this investigation. It was found that, for the measured field current of six nanoamperes (6 x 10^{-9} amperes), at $p/p_0 = 0.9$ and V = 6000 kV, the resulting increase in temperature is predicted to be only 0.195 °C (0.35 °F) over a five minute period. Based on the finding that the temperature increases as the adsorption rate increases in the presence of an electric field, it is felt that the temperature rises found throughout this work are the direct result of the heat of adsorption and therefore, the adsorption rate.

Because of the higher adsorption rates in the presence of an electric field, and in light of the fact

that the total amount adsorbed is constant, it follows that the adsorption rates will diminish more rapidly following the prolonged application of the field than would be expected without the field. The increased adsorption rates will invariably deposit more adsorbate in a shorter period of time and the driving force for the adsorption process will be reduced. Therefore, the rate of adsorption must be reduced because the total amount adsorbed is unchanged in the presence of an electric field. This may also indicate a relaxation in the system following prolonged application of the electric field similar to that observed by Dere'n and Mania (3) where catalytic reaction rates would increase in the presence of an electric field and then return to normal with the electric field still applied. Switching the electric field off and then reapplying it would again cause the reaction rate to increase.

The similarity of the temperature history curves at $p/p_0 = 0.7$ indicate that the electric field has little effect on the adsorption rate at this gas isostere (constant adsorbate concentration). This is felt to be due to the fact that only a few layers of adsorption occur at this adsorbate concentration. Furthermore, throughout the course of this investigation at $p/p_0 = 0.7$, it was noticed that small errors in the adjustment of the flowrate resulted in large deviations in the temperature profile data. For example, if the damp flowrate were adjusted a small amount too high $(p/p_0 = 0.75$ instead of 0.7 or a 7%

error), the temperature profile in the presence of a 6 kV electric field would deviate greatly from the expected profile and appear much like a $p/p_0 = 0.8$ profile exhibiting adsorption enhancement. Because of the rapid changes around the $p/p_0 = 0.7$ isostere, it is felt that this indicates the onset of multilayer adsorption.

In essence, the analysis presented by this thesis illustrates that adsorption rate enhancement in the presence of an electric field is not due to a silica gel temperature rise caused by the application of the electric field, which would in turn enhance the diffusion. logic followed to this conclusion is as follows: There was no appreciable temperature rise in the silica gel with dry air flowing through the sample in the presence of a 6 kV DC electric field. However, with damp sample air flowing and the 6 kV DC electric field applied, the silica gel temperature increased as compared to the non-field case. Therefore the increased temperature, based on the heat of adsorption term in the energy balance $(\dot{m}_{ads}\Delta H_{ads})$, is due to the increased adsorption rate. It is also possible that a change in the heat of adsorption in the presence of the electric field is at least partially responsible for the temperature increase. However, this is unlikely.

Quantitatively, the silica gel temperature increase due to the electric field is also shown to be small. The temperature rise due to the heat of adsorption during the first five minutes of an experiment with $p/p_0 = 0.9$ is

calculated to be 4.67 °C (see Appendix A). The temperature contribution of the 6 nanoamps of field current over a 5 minute period is 0.195 °C (see Appendix E). temperature rise due to the electric field is very small when compared to the adsorption related temperature rise. Furthermore, as the experiment continues, the field current increases. However, as evidenced by Figures 4.3, 4.4 and 4.5, the silica gel temperature in the presence of a 6 kV electrical field is less than in the non-field conditions for experimental times greater than 15 minutes. Therefore, the initial enhanced adsorption rate in the presence of the electric field results in lower adsorption rates later in the experiment. The field adsorption rates decrease below the non-field adsorption rates enough to more than compensate for the increased heat generated by the electric field.

Although the application of the electric field may affect the diffusion in the silica gel pores, the adsorption rate increase, found by Someshwar (20) in the presence of an electric field, was not due to a temperature rise in the silica gel sample caused by the application of the external electric field.

B. Discussion of Results for S-4133 Silica Gel

Someshwar (20) found increased adsortion rates in the presence of a 6 kV electric field for S-4133 silica gel also. Temperature studies on this silica gel were

performed in the absence of an electric field and in the presence of a 3.5 kV electric field. The results of this investigation show no discernible difference between the two cases. Apparently the electric field of 3.5 kV is not sufficient enough to interfere with or overcome the already strong interaction between the silica gel surface and the water vapor. This information is used to support the finding by Someshwar that adsorption enhancement did not occur in electric fields below 6 kV. The temperature history curve of the field case for this silica gel remains higher than the non-field case because the adsorption rates are similar due to the absence of any enhancement but, the field curve possesses a small field current to maintain its higher temperature. At the measured field current of 20 nanoamperes at 3.5 kV, the field contribution to the silica gel temperature is 0.076 °C/min. This approximates the temperature difference between the field and non-field cases shown in Figure 4.6 quite well.

Chapter VI

Conclusions

The various conclusions reached during this investigation are listed below:

- 1. The initial rate of adsorption of water vapor onto S-2509 Silica Gel is greater in the presence of a 6 kV electric field with $p/p_0 = 0.7$, 0.8 or 0.9.
- 2. The previous assumption of isothermal conditions for water vapor adsorption onto silica gel samples of approximately 50 to 60 milligrams is not totally justified, as shown by the 3 to 4 °C temperature rises found during this phase of the research.
- 3. The temperature rises found during the adsorption process are primarily the result of the heat of adsorption and not due to the flow of current in the electric field. The field current contributed a maximum temperature rise of 0.195 $^{\circ}$ C during the first five minutes of experimentation at $p/p_{\circ} = 0.9$.
- 4. The high initial rate of adsorption produces an abrupt temperature rise followed by convective cooling by the adsorbate carrier gas.

- 5. The adsorption rate of water vapor onto silica gel in the absence of an electric field is a direct function of the adsorbate concentration gradient between the influent gas and the adsorbent surface.
- 6. The maximum temperature rise of the silica gel in the absence of an electric field is a direct function of the adsorbate concentration of the influent gas.
- The initial adsorption rates at $p/p_0 = 0.8$ and 0.9 7. are approximately equal in the presence of a 6 kV electric field. Although the gas phase adsorbate concentrations are different, the presence of the electric field enhances the adsorption rate of the less concentrated stream to a value coinciding with the more saturated stream. In essence, the 6 kV electric field increases both adsorption rates, but the rate at $p/p_0 = 0.8$ is increased by a greater amount to a limiting value bounded by the adsorption rate of the more saturated stream at the experimental conditions. The adsorption rates at the two p/p concentrations appear limited by the changes in the gas concentration during the high rate process and thus are diffusion controlled at high p/p values.

- 8. The reasonably accurate prediction of the silica gel temperature rise using the energy balance indicates that the heat of adsorption is not changing due to the presence of an electric field. This illustrates that little or no change is occurring in the physical adsorption process. This change would be evidenced by the heat of adsorption or by the activation energy values in the presence of a 6 kV electric field differing from the corresponding values in the absence of the electric field. The work of Lincoln and Olinger (16), finding heat of adsorption differences, and the work of Keier, Mikheeva and Usol'tseva (10), finding activation energy changes, in the presence of electric fields supports the potential for these changes to occur. However, it is unlikely that this is the case for this thesis.
- 9. The isotere of $p/p_0 = 0.7$ is the approximate point where the first few layers of adsorbed material is completed and significant multilayer adsorption begins.
- 10. Adsorption enhancement, as indicated by the temperature studies, does not occur in an electric field of 3.5 kV magnitude on S-4133 Sigma Chemical Silica Gel. It is possible that adsorption enhancement does occur, but that the rate increase is small and therefore the heat transfer dominates.

- 11. Temperature increase can be used as an indicator that adsorption is occurring. By employing strict system conditions, it would be possible to calibrate a flow system to employ temperature increase as an absolute measurement of adsorption rate.
- 12. The increase in temperature in this system is the result of the adsorption rate and the heat of adsorption. This can be seen by examining the large positive term in the energy balance of mads △Hads. (Appendix B demonstrates the use of this term). The converse: the increase in temperature enhancing the mass transfer rate and thus appearing as enhanced adsorption is untrue.
- 13. The adsorption enhancement in the silica gel may possibly be only a temporary phenomenon. Relaxation within the system may reduce the effect of the electric field over long periods of time (see Figures 4.3 and 4.4). The field temperature curves for p/p₀ = 0.8 and 0.9 will initially increase very rapidly and then actually fall below the non-field curve, due to the decreased driving force for adsorption, which results from the high initial adsorption rate in the presence of an electric field. A relaxation effect was seen in the work of Dere'n and Mania (3) where the catalytic reaction rate would increase in the

presence of an electric field and then return to normal with the electric field still applied. This is a possible explanation.

Chapter VII

Recommendations

The purpose of this section of the thesis is to propose recommendations for additional study and to propose improvements in the methods used to obtain the results of this thesis. The following are suggestions for continued and improved study:

1. Although weighing of the silica gel before and after experimental runs indicated that significant atmospheric water contamination was not occurring, further modifications of the experimental arrangement could be performed to completely remove the possibility of unwanted water adsorption. One method for obtaining this modification is to redesign the adsorption chamber as a cell capable of withstanding a vacuum. The silica gel sample could then be loaded into the adsorption chamber and a vacuum pump could be used to evacuate the chamber overnight. At the time of experimentation, the adsorption chamber could be removed from the vacuum pump with all of the openings in the chamber tightly The chamber would then be inserted into the experimental flow scheme and the experiment begun, bringing the silica gel atmospheric exposure to a

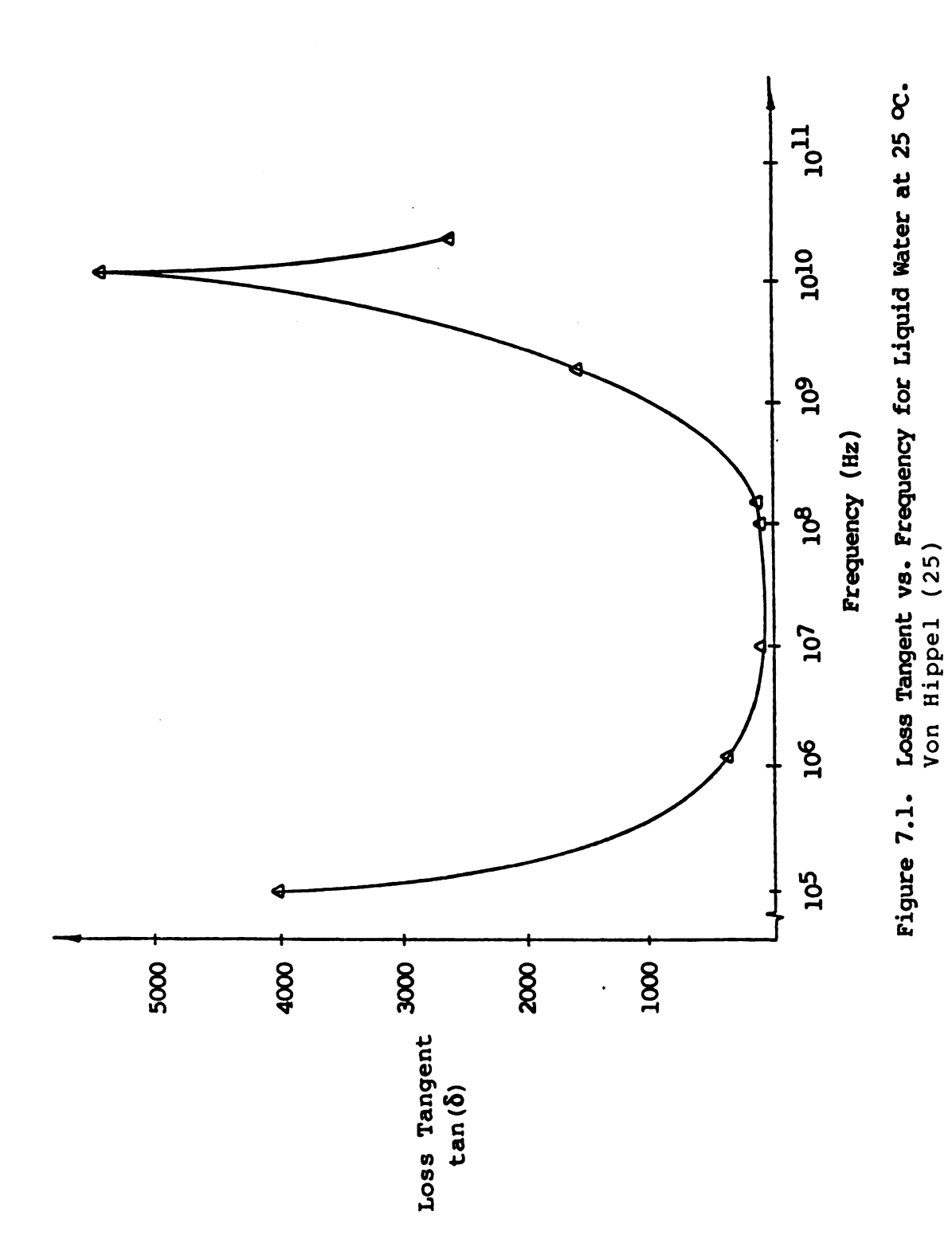
minimum.

- 2. The present experimentation indicated that the silica gel sample preparations of baking or evacuation were equally effective. To ensure total removal of adsorbed water from the silica gel, it is the recommendation of this thesis that the silica gel be baked in a 100°C to 130°C environment and then immediately placed in an evacuated chamber, preferably in the adsorption chamber described in item number one.
- 3. The work of Keier et al. (10) which found the results of the catalytic activity study to be a function of the polarity of the electric field used, suggests that reversal of the electric field polarity be investigated for water vapor adsorption on silica gel. This alteration could be completed with a minimum of rewiring and its affect studied quickly.
- 4. Studies should be performed to determine the duration of the adsorption rate enhancement in the presence of an electric field. In other words, does the adsorption rate enhancement occur immediately upon application of the field or at some measureable time following the application of the field? Also, this investigation should be extended to determine if the adsorption rate enhancement is a function of time. In essence,

investigate the adsorption enhancement phenomena for prolonged duration, cyclic duration or short duration and, following this, determine if the adsorption enhancement phenomena are a function of the experimental time.

- 5. In conjunction with recommendation number four, perform adsorption studies with the electric field on throughout the experiment and with the field being turned on at intermittent times. If a relaxation in the adsorption rate is found during constant application of the field, examine the silica gel system in the presence of cyclic application and removal of the external electric field. The work of Dere'n and Mania (3) found that catalytic oxidation rates returned to normal following prolonged application of an electric field. Also, upon removing the electric field and then reapplying it, the rate enhancement would again occur.
- adsorption enhancement is a function of the frequency of an A.C. electric field applied. Investigation of the dielectric constant of liquid water indicates a minimum in the value of the loss tangent at a frequency of 1 x 10⁷ cycles per second (25) (see Figure 7.1).

 The loss tangent of a dielectric is the ratio of loss

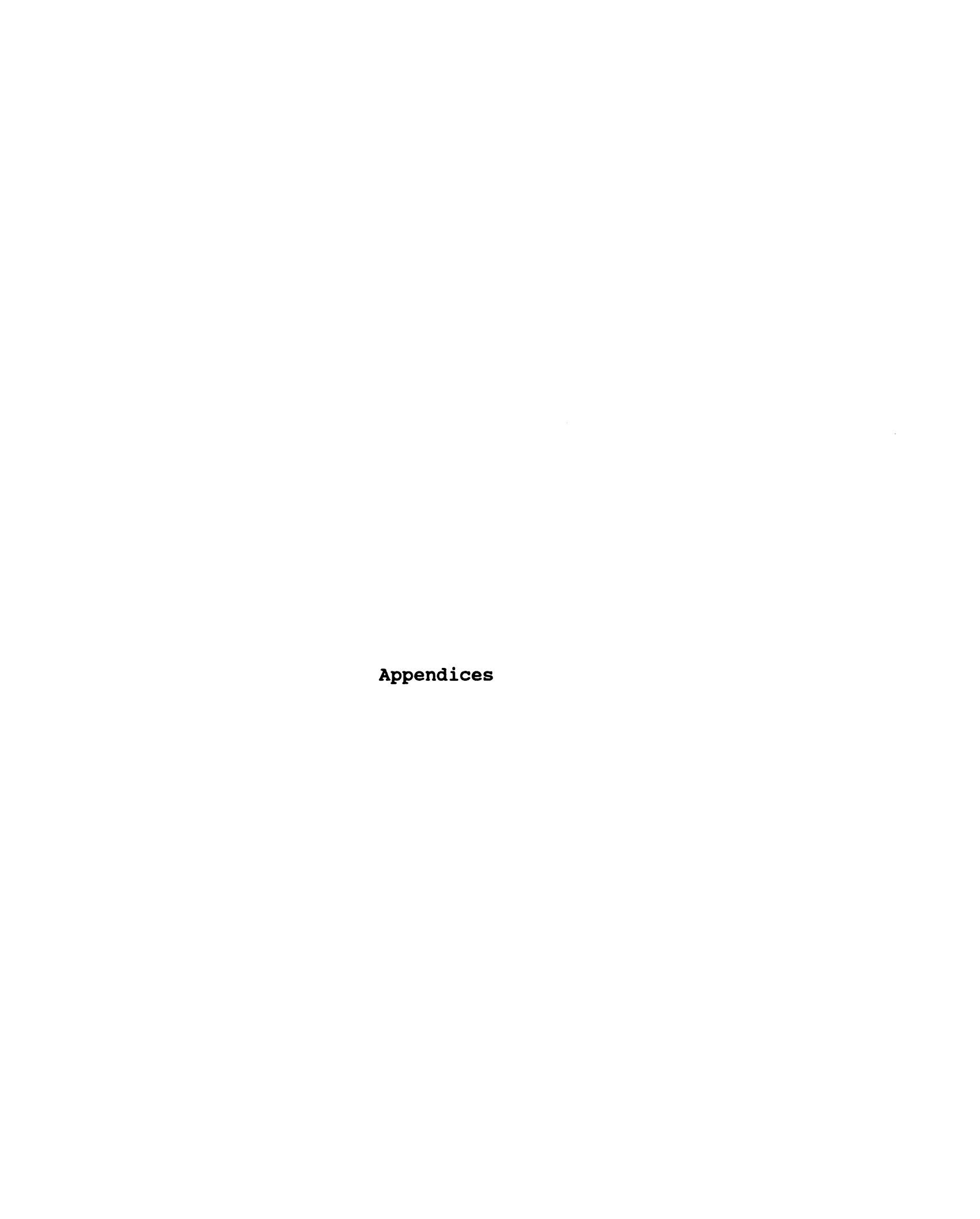


current to charging current also known as the dissipation factor, D. Because the loss tangent is a function of frequency, it is recommended that the effect of high frequency, low amplitude electromagnetic radiation on the silica gel sytem be investigated. The frequency of 1 x 10⁷ appears to be the most efficient for use with water adsorbate and would determine if the magnitude of the field voltage is necessary for adsorption enhancement or simply some threshold level of excitation.

- 7. Lincoln and Olinger (16) found that the influence of the electric field became less pronounced as the pressure of the system was increased. The effect of pressure on this system would provide information concerning the adsorbate diffusion rates in and out of the pores. This phenomenon should be investigated in the presence and absence of an electric field.
- 8. Determination of the heat of adsorption in the presence and absence of an electric field would yield insight into changes in the physical adsorption process.
- 9. The temperature history curves from this work indicate adsorption rate enhancement prior to the onset of multilayer adsorption. Also, the catalytic studies cited in this work show rate enhancement in the

presence of an electric field. Because surface catalysis is generally a chemisorptive phenomenon, the effect of the electric field appears to be between the adsorbate and the adsorbent. Someshwar found that the adsorption enhancement occurred during the multilayer portion of the adsorption process, which is an interaction between adsorbate in the liquid and gas phases. Because of this, a recommendation of this thesis is to study the effect of an electric field on condensation processes. This would yield insight into when the adsorption enhancement is occurring.

10. Accurately measure and record the electric field current in future experiments. This will yield insight into the duration of the field effect and will provide information for accurate and complete electric field heating calculations.





Appendix A Silica Gel Energy Balance

Energy Balance:

$$0 = \hat{m}_{ads} \triangle H_{ads} \triangle t + C_1 IV(\triangle t) - C_2 \hat{m}_{air} C_{pair} \triangle T_{air}(\triangle t) + m_{sq} C_{psq} \triangle T_{sq} - UA \triangle T_{sqa}(\triangle t).$$

mads = Adsorption rate of water onto silica gel

(mg water/min)

= Heat of adsorption (Btu/mg)
= Time (min)

c₁ c₂ I = Conversion constant 0.0569 Btu/min/watt = Conversion constant 3.968 x 10⁻³ Btu/cal

= DC field current (Amperes) = DC field voltage (Volts)

= Mass flow rate of moist air (mg/min)

C_{pair} = Specific heat of air (cal/mg °C)
ΔT_{air} = Temperature rise of moist air stream as it passes across silica gel sample (OC) (ATair calculation is found in Appendix C)

= Mass of silica gel sample (mg)

= Specific heat of silica gel (Btu/mg OF)
= Temperature change of silica gel (OF)

= Overall heat transfer coefficient and area
combination (Btu/min OF) (UA calculation is found in Appendix B)

 ΔT_{sqa} = Temperature difference between the silica gel and the air stream

Dividing by Δt and taking the limit as $\Delta t \rightarrow 0$ yields:

$$0 = \dot{m}_{ads} \triangle H_{ads} + C_{1}IV - C_{2}\dot{m}_{air}C_{pair}\triangle T_{air} - m_{sg}C_{psg}\frac{dT_{sg}}{dt}$$
$$- UA\triangle T_{sga}.$$

Rearrangement yields the final energy balance of:

$$m_{sg}c_{psg}^{dT_{sg}} = \dot{m}_{ads}^{\Delta H_{ads}} + c_{1}IV - c_{2}\dot{m}_{air}c_{pair}^{\Delta T_{air}} - UA\Delta T_{sga}.$$

The following calculation is employed to approximate the adiabatic temperature increase during the first five minutes of an experimental run.

Given: $p/p_0=0.9$, t=5 min, $\Delta T=4.1$ OC, E=6 kV and I=6 x 10^{-9} Amps

Let m = mg of H_2O adsorbed

 $Q_{ads} = (m) (6.348 \times 10^{-5} Btu/mg)$

 $Q_{CONV} = UA\Delta T$, where $\Delta T = (4.1+0)/2 = 2.05$ °C = 3.69 °F = (1.31 x 10⁻⁴ Btu/hr-°F) (3.69 °F) = (4.83 x 10⁻⁴ Btu/hr) (5 min) (1 hr/60 min) = 4.02 x 10⁻⁵ Btu/5 min

 Δ T Due to the electric field can be found using:

$$\Delta^{T}_{field} = \frac{(.0569Btu/min/Watt)}{(60 mg)(4.846 x 10^{-9} Btu/mg^{-0}F)} (6000 V)(5 min)}{(60 mg)(4.846 x 10^{-9} Btu/mg^{-0}F)}$$

 $Q_{accum} = {}^{m}sg^{C}psg^{\Delta T}rev$, where $\Delta T_{rev} = \Delta T_{experimental} - \Delta T_{field}$ = (60 mg) (4.846 x 10⁻⁷Btu/mg- ${}^{O}F$) ((4.1) (1.8) - 0.352) = 2.043 x 10⁻⁴ Btu in 5 minutes

Now, $Q_{ads} - Q_{conv} = Q_{accum}$ (6.348 x 10⁻⁵)m - 4.02 x 10⁻⁵ = 2.043 x 10⁻⁴

 $m = 3.85 \text{ mg H}_2\text{O}$ adsorbed in 5 minutes

$$\Delta^{\text{T}}_{\text{adiabatic}} = \frac{(6.348 \times 10^{-5})(3.85)}{(60)(4.846 \times 10^{-7})} = 8.41 \, ^{\text{O}}_{\text{F}} = 4.67 \, ^{\text{O}}_{\text{C}}$$

The temperature removed by convective heat transfer can be found as follows:

$$\Delta T_{\text{conv}} = \frac{(2.28 \times 10^{-6} \text{ Btu/min}^{-0}\text{F}) (2.05 ^{\circ}\text{C}) (1.8^{\circ}\text{F}/^{\circ}\text{C}) (5 \text{ min})}{(60 \text{ mg}) (4.846 \times 10^{-7} \text{ Btu/mg}^{-0}\text{F})}$$

$$= 1.45 ^{\circ}\text{F} = .81 ^{\circ}\text{C}$$

Therefore, the adiabatic temperature increase is 4.67 $^{\rm O}$ C, the experimentally measured temperature increase is 4.1 $^{\rm O}$ C and the non-adiabatic temperature increase is 3.86 $^{\rm O}$ C.



Appendix B Determination of UA from Experimental Data

By employing the portion of the silica gel verses temperature curve where it is nearly flat, i.e., t > 180 minutes, an approximation can be found for UA to be used in the energy balance equation. Originally, adsorption rates used in this calculation were EWLU data. When this data was found to be erroneous, adsorption rates were found using the slope of the total adsorption vs. time curves generated by Someshwar. (20) An example of this calculation is as follows:

$$\triangle H$$
 = 16 cal/gm = 6.3488 x 10⁻⁵ Btu/mg (17)
 C_{psg} = 0.22 Btu/lb-OF = 4.846 x 10⁻⁷ Btu/mg-OF (18)

For t = 180 min to t = 190 min $\dot{m}_{ads} = 0.0837 \text{ mg/min} \quad (\dot{m}_{ads} \text{ at } 185 \text{ min})$

$$\triangle T$$
 (due to \mathring{m}_{ads}) = $\frac{(\mathring{m}_{ads})(\triangle H_{ads})(\triangle t)}{(mass_{sg})(C_{psg})}$

$$= \frac{(0.0837 \text{ mg/min}) (6.3488 \times 10^{-5} \text{ Btu/mg}) (10 \text{min})}{(60 \text{ mg}) (4.846 \times 10^{-7} \text{ Btu/mg})}$$

$$=1.828$$
 $^{\circ}F = 1.0155$ $^{\circ}C$

mads = Adsorption rate of water onto silica gel (mg water/min)

∆H_{ads} = Heat of adsorption (Btu/mg) t = Time (min)

= Mass of silica gel sample (mg)

= Specific heat of silica gel (Btu/mg OF) Cpsq

From experimental data:

$$\triangle T$$
 at 180 min = 1.35 °C $\triangle T$ at 190 min = 1.32 °C $\triangle (\triangle T)$ = 0.03 °C = 0.054 °F $\triangle T_{avg}$ = 1.335 °C.

Heat load due to adsorption:

$$q_{ads} = (\dot{m}_{ads}) (\Delta H_{ads})$$

= (0.0837 mg/min) (6.3488 x 10⁻⁵ Btu/mg)
= 5.31 x 10⁻⁶ Btu/min.

Assuming that the heat load, q, is the same for the additional 0.03 °C (0.054 °F) temperature change,

$$q_{actual} = (1 + 0.054/1.828)(5.31x10^{-6} Btu/min).$$

= 5.47 x 10⁻⁶ Btu/min

Now, since $q = UA \triangle T$, then $UA = q / \triangle T$.

$$UA = \frac{5.47 \times 10^{-6} \text{ Btu/min}}{(1.335 \text{ °C})(1.8 \text{ °F/°C})}$$

$$= 2.28 \times 10^{-6} \text{ Btu/min-°F}$$

$$= 1.37 \times 10^{-4} \text{ Btu/hr-°F}$$

Repeated calculations for 10 minute intervals to t = 240 minutes yield an average

UA = 1.31 x 10^{-4} Btu/hr-OF

Verification for the value of UA was performed by employing the temperature rise information from the non-adsorption experiments. The experiments were performed to determine the effect of the DC electric field alone on the silica gel temperature, i.e., in the absence of adsorption. Therefore, the electric field was the only heat input to the silica gel system. This calculation uses the maximum silica gel temperature rise from the experimental data, 0.08 °C, and the measured electric field current of 1 nanoamp.

Q = UA
$$\triangle$$
T

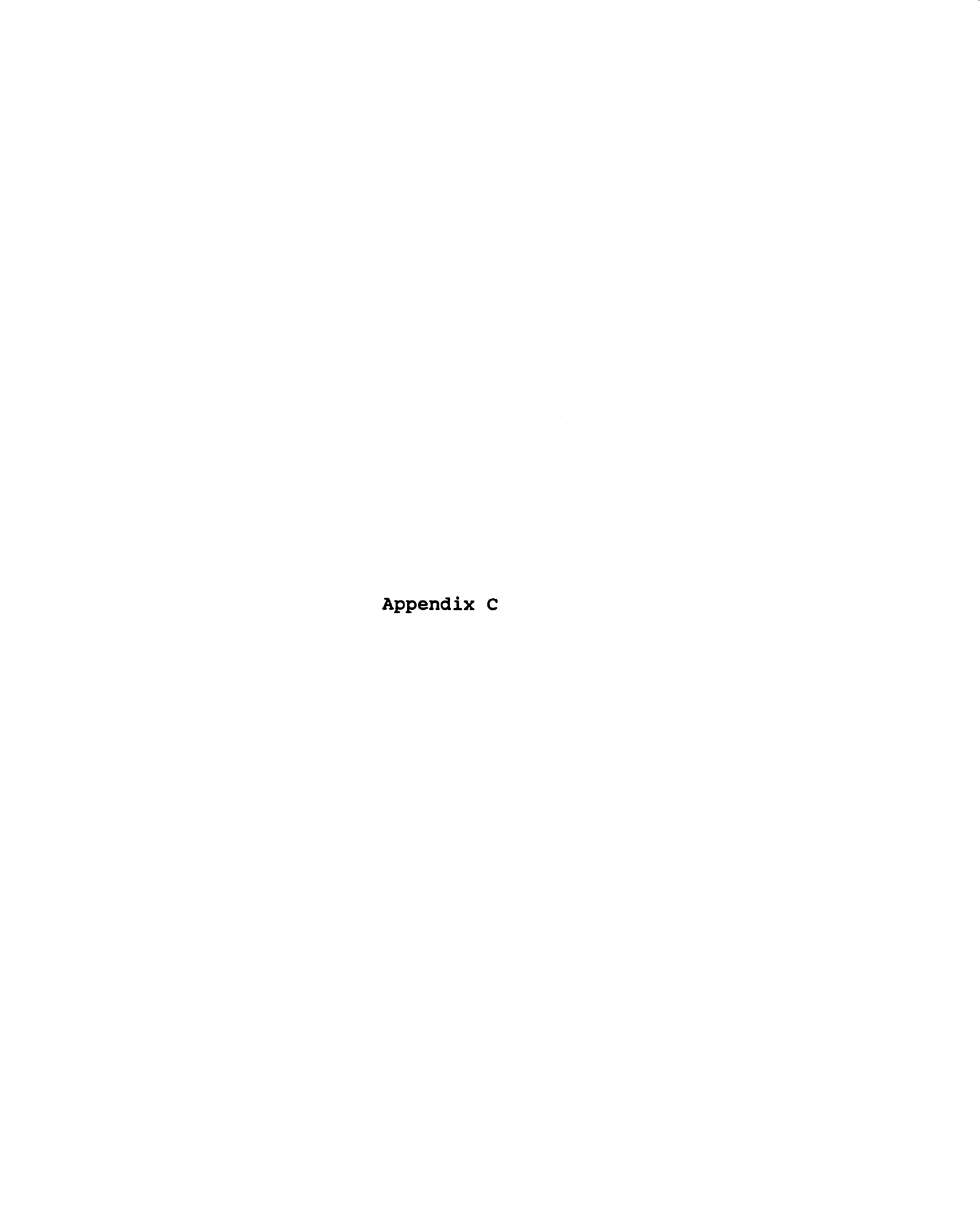
UA = Q/ \triangle T

= $\frac{(1X10^{-9} \text{ Amps}) (6000 \text{ Volts}) (0.0569 \text{ Btu/min/Watt})}{(0.08 \text{ °C}) (1.8 \text{ °F/°C})}$

= 2.37 X 10⁻⁶ Btu/min-°F

= 1.42 X 10⁻⁴ Btu/hr-°F

The value immediately above agrees favorably (within 9%) of the previously calculated value of 1.31 X 10^{-4} Btu/hr- $^{\circ}$ F.



Appendix C

Prediction of the Temperature Rise for the Moist Gas Stream

$$q = (m_{ads}) (\Delta H_{ads}) + IV(0.0569)$$

The highest temperature rise (worst case) will occur when the adsorption rate is the greatest, i.e., during the first five minutes of the adsorption experiment, and when the field current reached higher than normal levels. Typically the field current during the first five minutes of an experiment at $p/p_0 = 0.9$ was measured at six nanoamperes, however it was occasionally found to be 10 nanoamps. Therefore, to provide a worst case scenario, the highest values of adsorption rate and field current will be used in this calculation.

From t = 0 min to t = 5 min:

$$\dot{m}_{ads} = 0.509 \text{ mg/min}$$
 $V = 6000 \text{ Volts}$
 $I = 10 \times 10^{-8} \text{ Amps.}$

$$q = (0.509 \text{ mg/min}) (6.3488 \times 10^{-5} \text{ Btu/mg}) + (0.0569 \text{ Btu/min/Watt}) (1 \times 10^{-8} \text{ amps}) (6000 \text{ V})$$

$$= 3.232 \times 10^{-5} + 3.414 \times 10^{-6}$$
 Btu/min

$$= 3.573 \times 10^{-5} Btu/min$$

For moist air at the experimental conditions:

Since
$$q = \hat{m}_{air} C_p \Delta T$$
, then
$$\Delta T_{air} = q/(\hat{m}_{air} C_p) = (286 \text{ mg/min}) (8.47 \times 10^{-5} \text{ Btu/mg-}^{\circ}F)$$

$$\Delta T_{air} = 0.148 \text{ }^{\circ}F = .082 \text{ }^{\circ}C \text{ @ 10 nanoamps}$$

Employing the typical field current of 6 x 10^{-9} amps results in $\triangle T = 0.142$ OF = 0.079 OC.



Appendix D Calculation Showing How the Pressure Drop Across the EWLU Reduced p/p

Information for this calculation was taken from Figure 3-4, "Water Content of Air," page 3-69 of The Chemical Engineer's Handbook (19).

At p = 2 atm in the sample tubing ahead of the EWLU and T = 80 °F, there is 0.45 x 10^{-2} lbs water/lb air @ $p/p_0 = 0.9$.

At p = 1 atm and T = 80 $^{\circ}$ F, there is 1.98 x 10^{-2} lbs water/lb air when p/p_o = 0.9.

The pressure drop across the EWLU is 9 psi. The "Water Content of Air" curve is linear in this pressure and temperature range, yielding an interpolated water content at 20.4 psi (2 atm minus 9 psi) of 1.08 x 10^{-2} lbs water/lb air @ p/p₀ = 0.9.

Therefore, $p/p_0 = 0.9$ at 2 atm (29.4 psi) expands to $p/p_0 = 0.42$ at 20.4 psi and further expands to $p/p_0 = 0.23$ at 14.7 psi (1 atm).

This change in gas saturation due to the pressure drop across the EWLU resulted in erroneously low adsorption rate measurements during the experiments performed to determine adsorption rates. The temperature studies were performed with the EWLU removed from the flow scheme and therefore, the temperature studies are accurate.

Appendix E

Appendix E

Calculation Showing the Silica Gel Temperature Rise Due to the Electric Field in the Absence of Adsorption

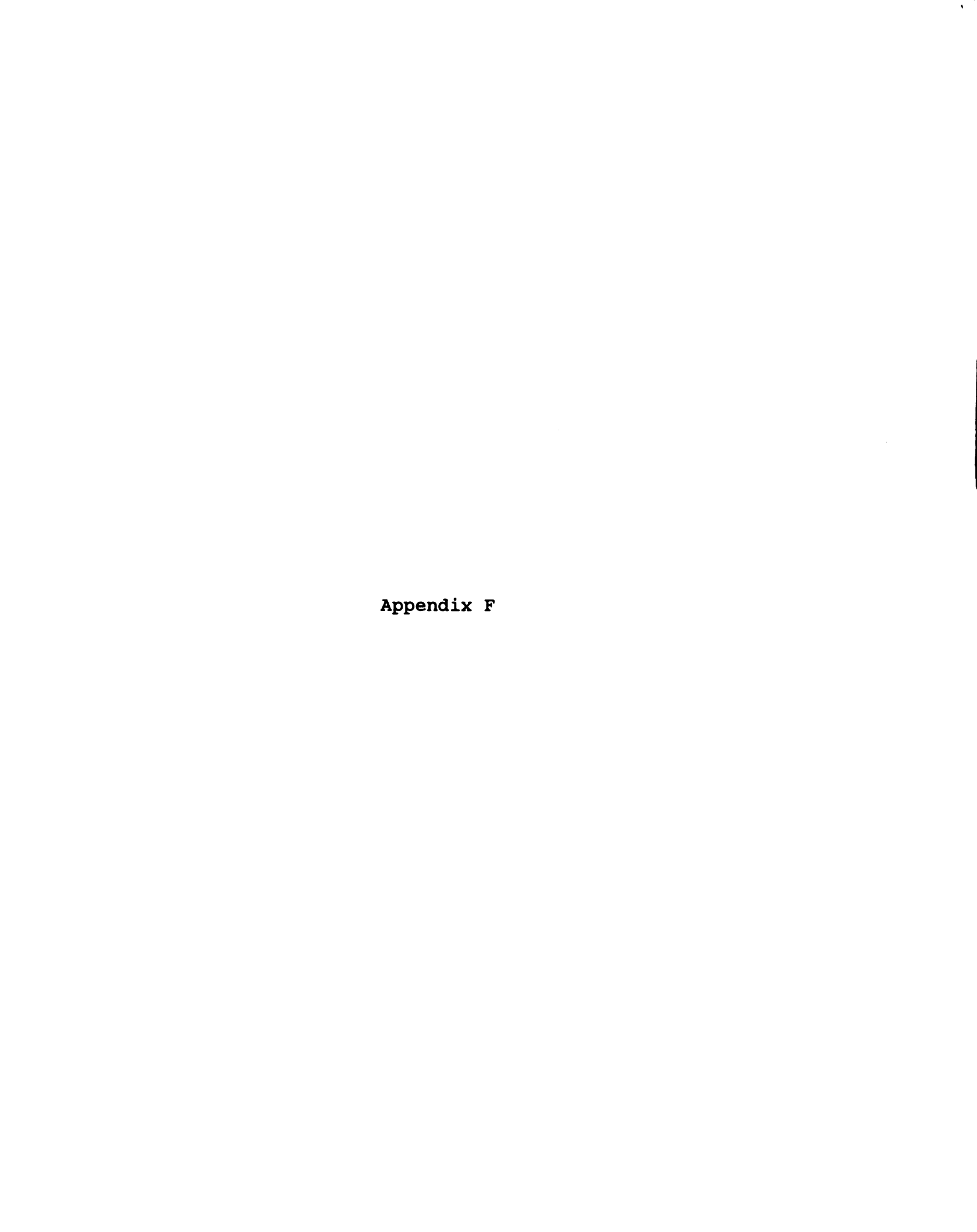
This calculation was performed to show the electric field contribution to the temperature rise of the silica gel sample. All terms in the energy balance are removed except for the electric field term. A field current of 6 nanoamperes was measured for experiments with $p/p_0 = 0.9$ during the first five minutes of adsorption. This current value is higher than the values found at $p/p_0 = 0.7$ or 0.8. The energy balance from Appendix A reduces to:

$$\Delta T = \frac{(0.0569 \text{ Btu/min/Watt}) (6 \times 10^{-9} \text{ amps}) (6000 \text{ V})}{(60 \text{ mg}) (4.846 \times 10^{-7} \text{ Btu/mg-°F})}$$

$$\Delta T = 0.07$$
 ^OF/min = 0.039 ^OC/min

In the absence of convective heat transfer, this temperature rise would convert to 0.35 °F (0.195 °C) over a five minute time span.

Experimental results from applying the electric field to a dry silica gel sample in the absence of adsorption yield the similar results.



Appendix F Raw Data

Non-Field Temperature Data

S-2509 Silica Gel-Unique Samples

V = 0 kV $p/p_0=0.7$

Used in Figures 4-1 and 4-5

Date: 7/12/85 Date: 7/13/85

Time (min)	ΔT (^O C)	Time (min)	ΔT (°C)
0		0	
5	1.80	5	1.61
10	2.15	10	2.08
15	2.16	15	2.15
20	2.11	20	2.12
25	2.02	25	2.05
30	1.78	30	1.99
35	1.65	35	1.94
40	1.55	40	1.88
45	1.47	45	1.83
50	1.40	50	1.77
55	1.35	55	1.70
60	1.29	60	1.65
70	1.24	70	1.57
80	1.20	80	1.48
90	1.16	90	1.41
100	1.12	100	
110	1.08	110	1.28
120	1.04	120	1.23

Non-Field Temperature Data

S-2509 Silica Gel-Unique Samples

V = 0 kV $p/p_0=0.8$

Used for Figures 4-1 and 4-4

Date: 7/3/85		Date: 7/10/85		Date: 7/10/85	
Time (min) <u>AT</u> (°C)	Time (min)	ΔT (°C)	Time (min	<u>Δτ (°c)</u>
0		0		0	
5	2.62	5	2.62	5	
10	2.77	10	2.87	10	2.93
15	2.64	15	2.78	15	2.82
20	2.48	20	2.65	20	2.63
25	2.33	25	2.53	25	2.47
30	2.28	30	2.44	30	2.36
35	2.22	35	2.33	35	2.27
40	2.11	40	2.27	40	2.20
45	2.02	45	2.20	45	2.13
50	1.97	50	2.13	50	2.09
55	1.88	55	2.16	55	2.05
60	1.86	60	2.16	60	2.02
70	1.77	70	1.93	70	1.98
80	1.68	80	1.58	80	1.85
90	1.59	90	1.45	90	1.53
100	1.53	100	1.36	100	1.33
110	1.44	110	1.31	110	1.23
120	1.33	120	1.27	120	1.20

Non-Field Temperature Data

S-2509 Silica Gel-Unique Samples

V = 0 kV $p/p_0=0.9$

Used for Figures 4-1 and 4-3

Dat	e: 6/	27/85	Date: 6/2	8/85	Date: 6/3	0/85
Time	(min)	ΔT (^O C)	Time (min)	<u>ΔΤ (°C)</u>	Time (min)	ΔT (OC)
	0		0		0	
	5	2.80	5	2.33	5	2.33
1	.0	3.04	10	2.83	10	2.96
	.5	3.28	15	2.91	15	3.00
2	0	2.94	20	2.83	20	2.93
2	5	2.72	25	2.74	25	2.84
3	0	2.53	30	2.65	30	2.76
3	5	2.33	35	2.58	35	2.67
4	0	2.19	40	2.53	40	2.60
4	5	2.04	45	2.45	45	2.53
5	0	2.01	50	2.40	50	2.47
5	55	1.95	55	2.36	55	2.42
6	0	1.90	60	2.33	60	2.35
7	0	1.81	70	2.25	70	2.27
8	0	1.75	80	2.11	80	2.20
9	0	1.70	90	2.03	90	2.13
10	0	1.64	100	1.94	100	2.07
11	.0	1.61	110	1.87	110	1.98
12	0	1.55	120	1.82	120	1.91

Electric Field Temperature Data

S-2509 Silica Gel-Unique Samples

V = 6 kV $p/p_0=0.7$

Used for Figures 4-2 and 4-5

Date: 7/25/85		Date: 7/25/85		Date: 7/27/85	
Time (mi	in) <u>ot (</u> °c)	Time (min)	ΔT (°C)	Time (min)	<u> </u>
0		0		0	
5	2.35	5	2.29	5	2.36
10	2.50	10	2.45	10	2.45
15	2.26	15	2.23	15	2.28
20	2.10	20	2.12	20	2.05
25	1.92	25	2.05	25	1.88
30	1.79	30	1.96	30	1.76
35	1.68	35	1.85	35	1.65
40	1.57	40	1.81	40	1.56
45	1.50	45	1.72	45	1.47
50	1.45	50	1.69	50	1.41
55	1.39	55	1.63	55	1.34
60	1.35	60	1.58	60	1.27

V = 6 kV $p/p_0=0.8$

Used for Figures 4-2 and 4-4

Date: 7	/22/85	Date:	7/23/85	Date:	7/23/85
Time (min	<u>ΔΤ (°C)</u>	Time (min)	ΔT (°C)	Time (min)	ΔT (°C)
0		0		0	
5	4.06	5	4.06	5	3.86
10	3.46	10		10	3.26
15	2.85	15	2.87	15	2.71
20	2.57	20	2.41	20	2.25
25	2.34	25	2.18	25	2.16
30	2.17	30	1.94	30	1.58
35	2.01	35	1.78	35	1.75
40	1.86	40	1.67	40	1.65
45	1.75	45	1.56	45	1.58
50	1.68	50	1.47	50	1.58
55	1.57	55	1.38	55	1.40
60	1.48	60	1.36	60	1.36

Electric Field Temperature Data

S-2509 Silica Gel-Unique Samples

V = 6 kV $p/p_0=0.9$

Used for Figures 4-2 and 4-3

Date: 7/18/85 Date: 7/19/85 Date: 7/20/85

Time (min) <u>ot</u> (°c)	Time (min)	ΔT (°C)	Time (min)	ΔT (°C)
0		0		0	
5	4.28	5	3.94	5	4.06
10	3.56	10	3.60	10	3.62
15	2.75	15	2.82	15	3.08
20	2.57	20	2.66	20	2.80
25	2.39	25	2.62	25	2.68
30	2.29	30	2.46	30	2.69
35	2.19	35	2.53	35	2.55
40	2.08	40	2.31	40	2.31
45	1.95	45	2.26	45	2.26
50	1.94	50	2.20	50	2.20
55	1.90	55	2.19	55	2.17
60	1.83	60	2.20	60	1.82

Field and Non-Field Temperature Data

S-4133 Silica Gel-Unique Samples

 $p/p_0 = 0.9$

Used for Figure 4-6

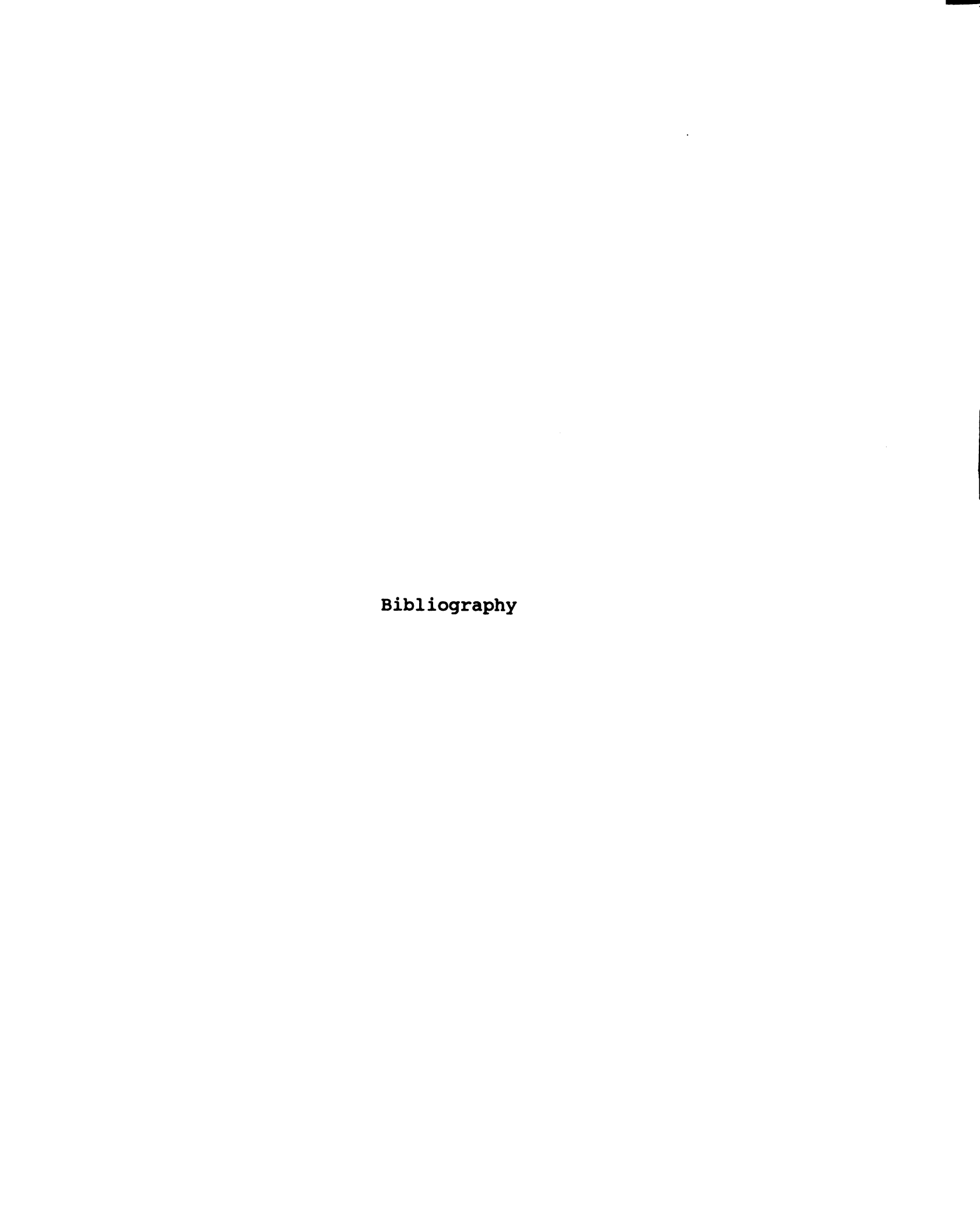
V = 0 kV

V = 3.5 kV

Date: 6/5/85

Date: 5/25/85

Time (min)	ΔT (^O C)	Time (min)	ΔT ($^{\circ}C$)
0		0	
5	2.77	5	2.30
10	3.19	10	3.20
15	3.17	15	3.30
20	3.03	20	3.21
25	2.86	25	3.09
30	2.70	30	2.94
35	2.57	35	2.81
40	2.43	40	2.65
45	2.28	45	2.54
50	2.04	50	2.41
55	1.99	55	2.29
60	1.90	60	2.19



BIBLIOGRAPHY

- 1. Adams, T., M. A. Steinmetz, D. B. Manner, D. M. Baldwin, and S. R. Heisey, "An Improved Method for Water Vapor Detection," <u>Annals of Biomedical</u>
 <u>Engineering</u>, Vol II, pp. 117-129, (1983).
- 2. Dere'n, Jerzy and Ryszard Mania, "Effect of an External Electric Field on the Oxidation of CO and CO₂ on a Nickel Oxide Catalyst," <u>Journal of Catalysis</u>, 35, pp. 369-375, (1974).
- 3. Dere'n, Jerzy and Ryszard Mania, "Relaxation Character of the Effect of External Electric Field on Kinetics of Oxidation of Carbon Monoxide on Zinc Oxide," Polish Journal of Chemistry, 48, pp 1565-1569, (1974).
- 4. Hasted, J. B., <u>Aqueous Dielectrics</u>, Chapman and Hall, London, (1973).
- 5. Hines, Anthony L. and Robert N. Maddox, <u>Mass Transfer</u>
 <u>Fundamentals and Applications</u>, Prentice-Hall Inc.,
 Englewood Cliffs, N.J., (1985).
- 6. Hoenig, Stuart and Freedoon Tamjidi, "Exo-electron Emission During Heterogeneous Catalysis (The Effect of External Electric Potentials)," <u>Journal of Catalysis</u>, 28, pp. 200-208, (1973).
- 7. Hoenig, Stuart and Mervin G. Utter, "Observations of Exoelectron Emission Associated with Heterogeneous Catalysis," <u>Journal of Catalysis</u>, 47, pp. 210-213, (1977).
- 8. Hsu, Woochun and V. J. Lee, "Electrodynamic Field Effect in Heterogeneous Catalysis and Kinetics: Hydrogenation of Benzene to Cyclohexane," Chemical Engineering Progress Symposium Series: Recent Advances in Kinetics and Catalysis, Vol 64, No. 89, pp. 12-17, (1968).
- 9. Iler, Ralph K. <u>The Chemistry of Silica</u>, John Wiley & Sons, New York, (1979).

- 10. Keier, N. P., E. P. Mikheeva and L. G. Usol'tseva, "Field Effect Study of the Relation Between the Fermi Level and the Catalytic Dehydration of Isopropyl Alcohol on TiO₂ Films," <u>Doklady Chemistry</u>: <u>Proceedings of the Academy of Sciences of the USSR</u>, Vol 182, No. 1, pp. 647-650, (1968).
- 11. Klein, S. M. and W. H. Abraham, "Adsorption of Ethanol and Water Vapors by Silicalite," <u>AICHE Symposium</u>
 Series: Adsorption and Ion Exchange, Vol 79, No. 230, pp. 53-58, (1983).
- 12. Kmiotek, S. J., Pingdong Wu and Y. H. Ma,
 "Simultaneous Measurements of Diffusion and Heat
 Effects During Sorption of Methanol in ZSM-5 Zeolite,"
 AICHE Symposium Series: Adsorption and Ion Exchange,
 Vol 78, No. 219, pp. 83-89, (1982).
- 13. Kooi, E. <u>The Surface Properties of Oxidized Silicon</u>, Springer-Verlag, New York, (1967).
- 14. Lee, H. and W. P. Cummings, "A New Design Method for Silica Gel Air Driers Under Nonisothermal Conditions," Chemical Engineering Progress Symposium Series, 74, 63, 42, (1967).
- 15. Lee, Vin-Jang, "Heterogeneous Catalysis: Effect of an Alternating Electric Field," <u>Science</u>, Vol 152, pp. 514, (1966).
- 16. Lincoln, W. W. and J. L. Olinger, "Enhancement of Gaseous Adsorption on Metal Surfaces Through the Use of an Applied AC Voltage," <u>AICHE Symposium Series</u>:

 <u>Adsorption and Ion Exchange</u>, No. 152, Vol 71, pp. 77-85, (1975).
- 17. Mantell, C. L. <u>Adsorption</u>, 1st Edition, McGraw-Hill Book Co., New York, pp. 155, (1945).
- 18. Mantell, C. L. <u>Adsorption</u>, 2nd Edition, McGraw-Hill Book Co., New York, pp. 176, (1951).
- 19. Perry, Robert H., ed., and Cecil H. Chilton, ed. <u>Chemical Engineers' Handbook</u>, 5th Edition, McGraw-Hill Book Co., New York, pp. 21-41, (1973).
- 20. Someshwar, A. V. "A Fundamental Study of the Effects of Applied Electric Fields on Gas-Solid (Dielectric) Adsorption" Ph.D. dissertation, Michigan State University, 1983.

- 21. Someshwar, A. V. and Bruce W. Wilkinson. "Study of Electric Field-Induced Effects on Water Vapor Adsorption in Porous Adsorbents," <u>Industrial and Engineering Chemistry Fundamentals</u>, Vol 224, pp. 215-220.
- 22. Stevens, Gregory, Data Analysis Computer Program, Michigan State University, 1984.
- 23. Treybal. Mass Transfer Operation, 3rd Edition, McGraw-Hill Book Co., pp. 574-575, (1980).
- 24. Vladov, D., V. L. Dyakovitch and S. H. Dinkov. "The Catalytic Decomposition of Ammonia: Electric Field Effect on the Catalytic Activity," <u>Journal of Catalysis</u>, 5, pp. 412-418, (1966).
- 25. Von Hippel, Arthur R., ed. <u>Dielectric Materials and Applications</u>, Wiley and Sons, Inc. New York, (1954).
- 26. Weast, Robert C., ed., and Melvin J. Astle, assoc. ed. <u>Handbook of Chemistry and Physics</u>, 63rd edition, CRC Press, Boca Raton, Florida, (1982).

